REVIEW

Electron spin resonance in the study of diamond

Rep. Prog. Phys., Vol. 41, 1978. Printed in Great Britain

Electron spin resonance in the study of diamond

JHN LOUBSER and JA VAN WYK

Department of Physics, University of the Witwatersrand, Johannesburg, South Africa

Abstract

The role of electron spin resonance in the study of both natural and synthetic diamond is reviewed in this article. A brief survey of the physical significance of the constants in the spin Hamiltonian, as well as experimental technique, is given. The review then deals in some detail with the various nitrogen centres found in diamond, treating exchange-interaction, Jahn–Teller and relaxation effects associated with these centres. Acceptor impurities and transition-ion impurities are briefly discussed. The rest of the review is then devoted to centres created by irradiation, subsequent heat treatment, mechanical deformation and ion implantation. The spin Hamiltonian parameters of these centres are tabled and the results are discussed within the framework of the defect molecule approach. In conclusion, the correlation between optical effects and the ESR measurements in the case of four defect centres are discussed in some detail as this seems to be a powerful method of testing the various models suggested for the observed defects. It is hoped that the tables given of the observed centres found in diamond up to the present will be useful to researchers in this field.

This review was received in December 1977.

0034-4885/78/0008-1201 $05.00

Contents

1. Introduction

1.1. Resonant absorption of electromagnetic radiation by unpaired electrons

The resonant absorption of electromagnetic radiation by unpaired electrons is known as electron spin resonance (ESR). An electron has a spin S of $\frac{1}{2}$ and an associated magnetic moment. Consequently, in a magnetic field the two spin states corresponding to the resolved spin $M_s = +\frac{1}{2}$ and $-\frac{1}{2}$ have different energies. Transitions may be caused between these states by a high-frequency magnetic field perpendicular to the steady field. In a field of 10 kG, the frequency is 28 000 MHz, which lies in the microwave region. Microwave energy can be absorbed when the quantum of microwave energy equals the spacing between the two levels, giving the basic resonance condition:

$$h\nu = g\beta H \tag{1.1}$$

where $\beta = (eh/2mc)$ is the Bohr magneton and $g = 2{\cdot}0023$ is the spectroscopic splitting factor for a free electron.

1.2. ESR as a probe for the detailed study of the nature of defects in semiconductors

Electron spin resonance is observed for electrons in a variety of situations. The ones which will concern us are (i) electrons localised at impurity atoms in the lattice of the solid, and (ii) unpaired electrons localised in orbitals at defect sites in solids. Such electrons are far from being free but are rather described by wavefunctions localised in a region of a discrete crystal lattice. The paramagnetism of these electrons reflects the interaction of the electrons with the lattice and we express this interaction in terms of the 'spin Hamiltonian'. For the defects in diamond the most commonly required spin Hamiltonian is one of the form:

$$\mathscr{H} = \beta \boldsymbol{H}.g.\boldsymbol{S} + \boldsymbol{S}.D.\boldsymbol{S} + \boldsymbol{S}.A.\boldsymbol{I}. \tag{1.2}$$

The first term represents the electronic Zeeman interaction, the second the interaction of the electron spin with the crystal field produced by the surroundings of the paramagnetic centre, and the last is the magnetic hyperfine interaction. S and I represent operators associated with electronic and nuclear spin respectively, and g, D and A are tensors to be determined experimentally. The second term is required only if the effective spin $S > \frac{1}{2}$. More will be said about these interactions in the next section.

Some features of ESR experiments are the following.

(i) Under favourable conditions with narrow lines, very small numbers (10^{10} cm^{-3}) of magnetic centres with $S = \frac{1}{2}$ can be detected at room temperature. There is usually an increase in sensitivity (proportional to $1/T$) at lower temperatures due to Boltzmann's distribution of spins.

(ii) Different types of paramagnetic centres in the same crystal normally give distinguishable microwave spectra.

(iii) The intensity of a particular centre indicates the number of centres of that type.

(iv) The shift of the spectroscopic splitting factor from the free spin value $\Delta g = g - 2{\cdot}0023$ is a measure of the orbital contribution to the magnetic moment and Δg is usually negative if the centre has unpaired electrons and positive if it has unpaired holes associated with it.

(v) If the effective spin is S there are $2S$ allowed transitions under normal conditions. These may be superimposed in the spectrum if the centre is in a surrounding of high symmetry but otherwise there are $2S$ separately resolved fine-structure lines, thus indicating the number of unpaired electrons associated with the defect.

(vi) Any nucleus of spin I associated with the defects splits each fine-structure line into $2I+1$ hyperfine components. Impurity defects with non-zero nuclear spins can thus be identified.

(vii) The anisotropy of the spectra as the crystal is rotated in the external magnetic field gives information about the symmetry of the defect. The magnitude of the isotropic part of the hyperfine splitting, usually denoted by O, is a measure of the time spent by the unpaired electron near a particular nucleus. It is thus possible to plot out the electron distribution. The 1·1% abundant ^{13}C atoms which have a nuclear spin of $I=\frac{1}{2}$ will give rise to weak satellite lines which give valuable clues as to the symmetry of the immediate surroundings of the defect.

(viii) The widths of the lines give information about magnetic and exchange interactions between defects and about spin–lattice relaxation effects.

Since the initial report of Zavoisky in 1945, electron spin resonance has been extensively studied, and excellent books on the subject are available (Low 1960, Pake 1962, Abragam and Bleaney 1970).

In this article the application of electron spin resonance techniques to natural and synthetic diamonds will be reviewed, as well as to centres in irradiated diamonds. Earlier reviews usually treated diamonds only very briefly as an example of just another semiconductor, e.g. Ludwig and Woodbury (1962) and Corbett (1966). Owen's (1965) review dealt mainly with irradiation-produced defects in diamond. Since then a considerable number of papers has appeared and many new centres have been observed.

1.3. Why study diamond?

Semiconductors with the diamond structure have the following characteristics in common which make them particularly interesting subjects for resonance study.

(i) They are intrinsically diamagnetic and show no cooperative phenomena such as ferromagnetism and antiferromagnetism.

(ii) Crystals which are studied are typically dilute in magnetically active impurities and have narrow resonance lines.

(iii) The tetrahedral symmetry about each lattice site and the simplicity of the lattice have facilitated the theoretical treatment of resonance and other phenomena. Part of the diamond lattice in the vicinity of a substitutional nitrogen impurity is shown in figure 1. Silicon, germanium and related group IV elements and compounds, InSb and related III–V compounds and ZnS and related II–VI compounds have been extensively studied (Watkins 1975). Diamond, on the other hand, has been studied in far less detail, mainly because of the inability to selectively dope diamonds. Natural diamonds had to be used, and without knowledge of the nature and amount of impurities in them this has led to a considerable amount of speculation and guessing about the observed spectra in natural diamonds, as well as electron- and neutron-irradiated

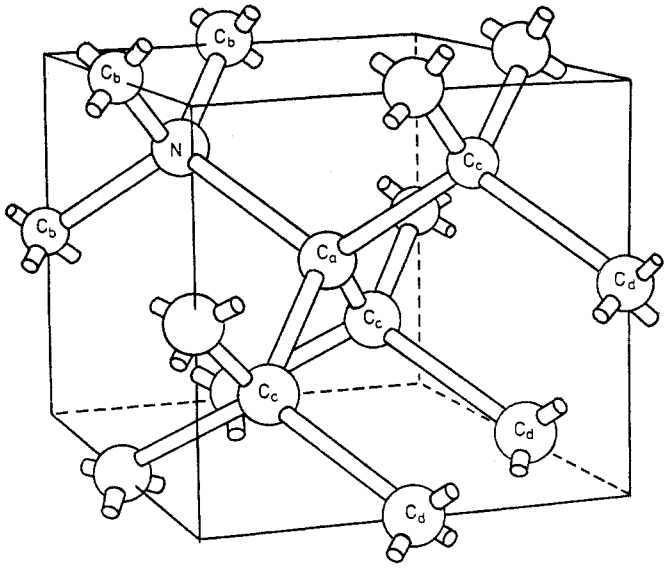

Figure 1. Part of diamond lattice in the vicinity of a substitutional nitrogen.

stones. The earlier expectation that synthetically grown diamonds doped with boron, aluminium, etc, would yield the answers has not materialised mainly because of the difficulty in controlling the doping and the ever-present magnetic impurities in the diamonds, causing the resonance lines to be broad and featureless.

Nevertheless the purely covalent nature of the tetrahedrally directed bonds resulting from the hybridisation of the atomic s and p orbitals of the carbon atoms makes it worthwhile to study diamond in depth.

Electrical, optical and other properties of diamond are very sensitive to small amounts of impurities. Spin resonance is one of the most sensitive and powerful tools for investigating the detailed nature of impurity sites. It is also possible to study one impurity in the presence of much larger concentrations of other impurities. This is rarely possible with other techniques.

Irradiation of semiconductors with electrons and neutrons produces vacancies and interstitials and aggregations of these defects as well as aggregations with impurities. In the identification of these defects, the understanding of how the defects are introduced (and removed) and the understanding of the changes in the physical properties caused by these defects, electron spin resonance has played a major role in the case of silicon and germanium. In diamond, the progress in this field has also been slower and the identification of defects and the formulation of acceptable models for the observed defect are by no means so far advanced as in the case of silicon, ZnS, etc. However, due to the unique properties of diamond (hardness, high Debye temperature, large refractive index, large forbidden gap (5·7 eV)), the further study of diamond using as many different techniques as possible will undoubtedly continue apace.

1.4. Nomenclature of ESR *centres in diamond*

The labelling system which has been adopted for ESR in irradiated silicon and germanium was suggested by Watkins (1965) and will be only slightly modified for

diamond. All ESR systems in diamond will be designated by the initial letter of the laboratory where it was discovered, followed by a number indicating the order of discovery as nearly as possible. No distinction is thus made between systems occurring in un-irradiated and irradiated diamond or in natural and synthetic diamond.

We will also follow Watkins in labelling the principal axes. The major axes will be designated with a subscript 1, whereas the minor axes will be labelled 2 and 3. The directions of these principal axes will be specified relative to the axes shown in figure 2.

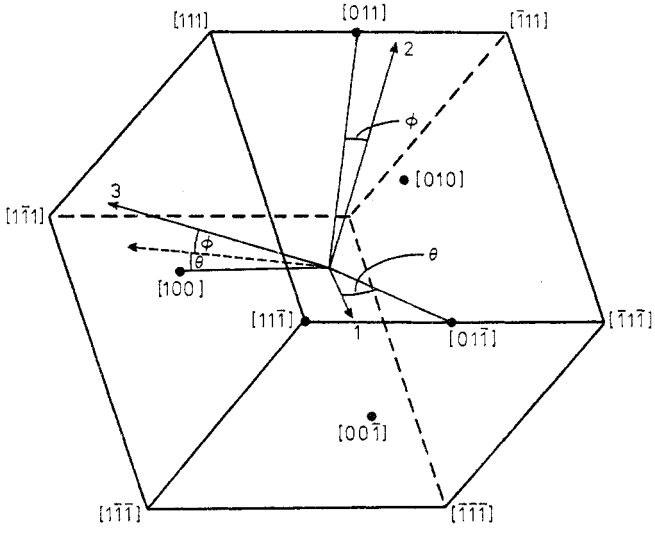

Figure 2. Principal axes of any tensor are obtained by a rotation about a [011] axis from [01$\bar{1}$] to [100] through an angle θ followed by a rotation about the new axis 1 through an angle ϕ.

2. The resonance technique

2.1. The spin Hamiltonian

The form of the spin Hamiltonian (1.2) for particular cases largely depends on the symmetry of the crystal field produced by the surroundings of the paramagnetic centre. For cubic symmetry:

$$g_1=g_2=g_3=g \qquad A_1=A_2=A_3=A \qquad D_1=D_2=D_3=0.$$

For cases of axial symmetry only the minor components of the tensors will be equal, and we write, for example, $g_{\parallel}=g_1$ and $g_{\perp}=g_2=g_3$. For lower symmetries all principal values will be different. In general, then, the symmetry of the Hamiltonian which describes the resonance data of the unpaired electrons associated with a particular defect give sensitive, qualitative data of any distortion from the regular arrangement of the surrounding diamagnetic ions. In diamond, where each atom is tetrahedrally surrounded by four other atoms, an impurity atom or a vacancy must also be surrounded by four carbon atoms, but tetrahedral symmetry need no longer be preserved due to the Jahn–Teller effect. The symmetry of the surroundings then drops from T_d to C_{3v}

symmetry and in more complicated systems, like a vacancy next to an impurity atom, to C_{2v} and to even lower symmetry for more complex aggregates of defects.

The hyperfine term is due to the coupling of the magnetic moments of the electrons and the nuclei. There are two forms of coupling (see, for example, Abragam and Pryce 1951). The isotropic hyperfine coupling or contact interaction term is given by

$$\mathscr{H}_1=\frac{8\pi}{3}g\beta g_n\beta_n|\psi(0)|^2\,\boldsymbol{I}.\boldsymbol{S} \tag{2.1}$$

and the anisotropic dipolar interaction is given by

$$\mathscr{H}_2=-g\beta g_n\beta_n\left(\frac{\boldsymbol{I}.\boldsymbol{S}}{r^3}-3\frac{(\boldsymbol{I}.\boldsymbol{r})(\boldsymbol{S}.\boldsymbol{r})}{r^5}\right) \tag{2.2}$$

where g_n is the nuclear g factor and β_n is the nuclear magneton.

The contact interaction can only occur when the electron has a finite probability density at the nucleus, i.e. the electron must have some s-orbital character. The dipolar interaction, on the other hand, will be zero for a spherical electron cloud and hence can only have a value if the electron has p, d, f or higher orbital character. For axial symmetry which is very common in diamond with its high degree of symmetry it can be shown (Smith *et al* 1959b) that

$$A_{\parallel}=g\beta g_n\beta_n(O+2P) \qquad A_{\perp}=g\beta g_n\beta_n(O-P) \tag{2.3}$$

where $O=(8\pi/3)|\psi(0)|^2$ represents the isotropic contribution, i.e. the s-character contribution and $P=\langle[z^2-\frac{1}{2}(x^2+y^2)]/r^5\rangle$ for p, d or f character contribution to the hyperfine coupling. If all except the s- and p-orbital contributions are neglected, it is possible to get an idea of the spin density distribution around a defect centre. This is a fairly good approximation in the case of diamond as the carbon atom bonds have s and p atomic orbitals easily available for bonds, while the d orbital is very much higher in energy. Consider a defect where the unpaired electron occupies an orbital built from atomic s and p orbitals. Suppose that this normalised molecular orbital is of the form:

$$\psi=c_s\psi_s+c_p\psi_p \tag{2.4}$$

where ψ_s and ψ_p are the s and p orbitals just discussed. If overlap is neglected the amount of s orbital involved is c_s^2 and the amount of p orbital involved c_p^2. If we know that an s-orbital electron in the free atom gives an isotropic splitting of O^* G and we observe an isotropic splitting O G then an estimate of the amount of unpaired electrons in the s orbital of the molecular orbital is given by

$$c_s^2=O/O^*.$$

Similarly, if there is an anisotropic contribution of P G and it is known that in the hypothetical atom having unit occupancy of the particular p orbital involved the value of the dipolar coupling is P^* G, then the amount of the electron in the p orbital on the magnetic nucleus is

$$c_p^2=P/P^*.$$

The free-atom values of O^* and P^* are generally not known from experiment but may be calculated with moderate accuracy from self-consistent-field wavefunctions (Ramsey 1953, Watson and Freeman 1961a, b, Atkins and Symons 1967).

Further information can be obtained from the hybridisation ratio $\lambda = c_p^2/c_s^2$. Coulson (1952) has shown that if one assumes that the bonds formed from the hybridisation of s and p orbitals on an atom are orthogonal to each other, then it is possible to estimate the bond angle from the hybridisation ratio.

The D term in the spin Hamiltonian when $S > \frac{1}{2}$ can be caused by several different types of interactions. For organic molecules in a triplet state, D is normally caused by dipole–dipole interaction between the two electrons, and the term which has to be added to the effective Hamiltonian is of the type $\mathscr{H}_D = \boldsymbol{S}.D.\boldsymbol{S}$ where D is a symmetric tensor. In terms of the principal axes which diagonalise the zero field tensor the Hamiltonian becomes:

$$\mathscr{H}_D = D_1 S_z^2 + D_2 S_x^2 + D_3 S_y^2. \tag{2.5}$$

However, as the tensor is traceless this can also be written as:

$$\mathscr{H}_D = D[S_z^2 - \tfrac{1}{3}S(S+1)] + E(S_x^2 - S_y^2) \tag{2.6}$$

where $D = \frac{3}{2} D_1$ and $E = \frac{1}{2}(D_2 - D_3)$.

In contrast, the zero field splitting in transition-metal ions usually arises because of spin–orbit coupling and in some cases can be so large that electron resonance cannot be observed. The spin–orbit coupling leads to an indirect electron spin–spin coupling. According to second-order perturbation theory this electronic energy contains a term:

$$-\xi^2 \sum_n \frac{\langle 0 \,|\boldsymbol{L}.\boldsymbol{S}|\, n\rangle \langle n \,|\boldsymbol{L}.\boldsymbol{S}|\, 0\rangle}{E_n - E_0} \tag{2.7}$$

which can be reduced to the form:

$$\mathscr{H} = \boldsymbol{S}.D.\boldsymbol{S}$$

where D is a spin–spin coupling tensor. The components of this tensor are

$$D_{ik} = -\xi^2 \sum_n \frac{\langle \psi_0 \,|L_i|\, \psi_n\rangle \langle \psi_n \,|L_k|\, \psi_0\rangle}{E_n - E_0} \qquad i, k = x, y, z. \tag{2.8}$$

Here it has been assumed that ψ_0 is the ground state and ψ_n is one of the excited states of the system, E_0 and E_n are their respective energies and ξ is the spin–orbit coupling constant.

It was noted before that the g factor is, in general, a tensor and that it departs from the free spin value of 2·0023 because some orbital magnetism can be coupled back to the spin by means of the spin–orbit coupling. Apart from a numerical factor the same matrix elements that appear in the expression for D appear in the theory of the g factor.

There are other factors influencing the value of D in specific cases and the calculation of D is extremely difficult in most cases. It is, however, important to note that if the origin of D is purely direct spin–spin interaction, it has a value of

$$D = -\tfrac{3}{2} g^2 \beta^2 \langle 1/r^3 \rangle \tag{2.9}$$

where the average is over all possible positions of the two electrons. Using this expression it is possible to get an idea of where the two electrons are localised. Gouterman and Moffitt (1959) have made calculations of the D and E factors when the two

electrons are in p orbitals. If r is larger than $\sqrt{2}\,a$, the value of E will be small compared to D, where $a = 1{\cdot}54$ Å in diamond.

2.2. The spin resonance spectrum

A very brief explanation of how the energy levels of the ground state are found from a given spin Hamiltonian will be given.

Consider an impurity atom having a nuclear spin I with an unpaired electron with spin $S=\frac{1}{2}$ occupying a site of undisturbed tetrahedral symmetry representing, for example, a paramagnetic ion substituting for a carbon atom in the diamond. The spin Hamiltonian is

$$\mathscr{H}=g\beta \boldsymbol{H}.\boldsymbol{S}+A\boldsymbol{S}.\boldsymbol{I} \tag{2.10}$$

where g is isotropic because cubic symmetry has been assumed which also dictates an isotropic hyperfine coupling.

From perturbation theory carried out to first order assuming $g\beta \boldsymbol{H}.\boldsymbol{S}$ is the largest term in (2.10) the energy levels E_{Mm} are

$$E_{Mm}=g\beta HM+AMm$$

where M is the magnetic quantum number of the electrons and m is the magnetic quantum number of the nucleus. The level structure and allowed electron spin transitions between them are illustrated in figure 3 for the case $S=\frac{1}{2}$, $I=\frac{1}{2}$.

The ordinary electron resonance transitions are those in which the quantum number M of the electron changes while the nuclear quantum number m remains fixed, i.e. the electron's spin precession in the applied steady magnetic field is flipped, by applying an external oscillatory high-frequency field perpendicular to the steady magnetic field, without affecting that of the nuclear magnetic dipole. The energy absorbed in going from the state $|M-1, m\rangle$ to the state $|M, m\rangle$ is given by

$$h\nu=g\beta H+Am \tag{2.11}$$

where $m=+\frac{1}{2}$ or $m=-\frac{1}{2}$ in this case. This gives rise to two lines separated by A. Going to second-order perturbation adds a term of the order of $A^2/2h\nu$ to expression (2.11) and it can, unless A is large, usually be neglected. It has also been assumed

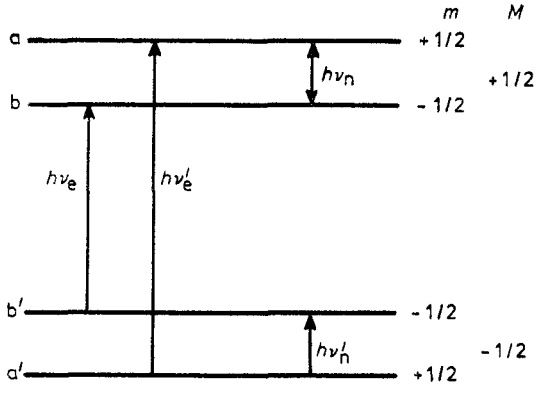

Figure 3. Energy-level diagram for the case $S=\frac{1}{2}$, $I=\frac{1}{2}$. The allowed transitions are indicated.

that the surrounding atoms have no nuclear magnetic moments. In the case of diamond there is a 4:90 chance that one of the four carbon atoms will be a ^{13}C atom with nuclear spin $I=\frac{1}{2}$. This will give rise to a pair of satellite lines associated with each hyperfine line. If the coupling of the 'free' electron to the 12 next nearest neighbours is large enough to be observed there will be two more satellites to each strong line closer in and with intensities three times that of the other pairs of satellites. Naturally, if the symmetry is lowered, i.e. if the electron does not spend equal times on the four nearest neighbours, the relative intensities of the various satellites will change.

2.3. Electron–nuclear double resonance

In some systems some or all of the hyperfine structure is not resolved. In these cases the electron–nuclear double resonance technique developed by Feher (1956) is very useful. It is essentially the observation of nuclear magnetic transitions via the electron spin resonance line. The technique is to use sufficient microwave power to saturate the electron line so that its intensity is greatly reduced, and then to enhance this line again by applying a nuclear resonance frequency which corresponds to the hyperfine splitting of the energy levels.

As an example, take the previous hypothetical case of a substitutional paramagnetic atom in the diamond lattice, with a free spin of $S=\frac{1}{2}$, and where the impurity atom had a nuclear spin of $I=\frac{1}{2}$. Figure 3 applies but now we include the nuclear Zeeman term in the spin Hamiltonian:

$$\mathcal{H}=g\beta \boldsymbol{H}.\boldsymbol{S}+A\boldsymbol{S}.\boldsymbol{I}-g_{\mathrm{n}}\beta_{\mathrm{n}}\boldsymbol{H}.\boldsymbol{I}. \tag{2.12}$$

If H is chosen so that $g\beta H \gg A$ and $g_{\mathrm{n}}\beta_{\mathrm{n}}H$, the energy levels in figure 3 will now be given to a good approximation by

$$\begin{aligned} E_{\mathrm{a,b}} &= \tfrac{1}{2}g\beta H \pm \tfrac{1}{4}A \mp \tfrac{1}{2}g_{\mathrm{n}}\beta_{\mathrm{n}}H \\ E_{\mathrm{a',b'}} &= -\tfrac{1}{2}g\beta H \mp \tfrac{1}{4}A \mp \tfrac{1}{2}g_{\mathrm{n}}\beta_{\mathrm{n}}H \end{aligned} \tag{2.13}$$

where the upper signs go with first subscripts.

The allowed electron spin transition a' $\rightarrow$ a ($\Delta M_I=0$) is now saturated by applying a resonating field whose energy is given by $h\nu_{\mathrm{e}}=g\beta H \pm \frac{1}{2}A$ so that the populations of a and a' are nearly equalised and the absorption intensity of the ESR line is drastically reduced. A slowly variable nuclear resonance frequency ν_{n} of order $\frac{1}{2}A/h$ is now applied and when $h\nu_{\mathrm{n}}=\frac{1}{2}A-g_{\mathrm{n}}\beta_{\mathrm{n}}H$ the nuclear transition a $\rightarrow$ b occurs so that a is depopulated into b and the electron resonance signal a' $\rightarrow$ a is restored in intensity. Similarly the transition a' $\rightarrow$ b' with energy $h\nu_{\mathrm{n}}'=\frac{1}{2}A+g_{\mathrm{n}}\beta_{\mathrm{n}}H$ can be measured via the intensity of the electron resonance signal. Thus $\nu_{\mathrm{n}}+\nu_{\mathrm{n}}'=A/h$ and $\nu_{\mathrm{n}}'-\nu_{\mathrm{n}}=2\,g_{\mathrm{n}}\beta_{\mathrm{n}}H/h$.

If the electron resonance line can be saturated this ENDOR method enables the direct measurement of nuclear magnetic moments, very accurate measurement of the hyperfine constants, and in some cases hyperfine structure can be resolved which is obscured by the width of the electron resonance line.

In the cases where the nuclear spin of the nucleus is larger than $\frac{1}{2}$, the nucleus possesses a quadrupole moment and another term:

$$P[I_z^2-\tfrac{1}{3}I(I+1)]+P'(I_x^2-I_y^2)$$

representing the interaction of the quadrupole moments with the electric field gradient,

must be included. The value of P and P' can also be obtained from the double resonance experiments.

2.4. Experimental techniques

A simple form of electron spin resonance spectrometer is shown diagrammatically in figure 4. The klystron is a special valve oscillator which produces monochromatic microwave radiation. This radiation is then led down a rectangular copper pipe or waveguide via an isolator and an attenuator and three port circulators to a resonant metal cavity in the magnetic field. The sample to be examined is placed in this cavity

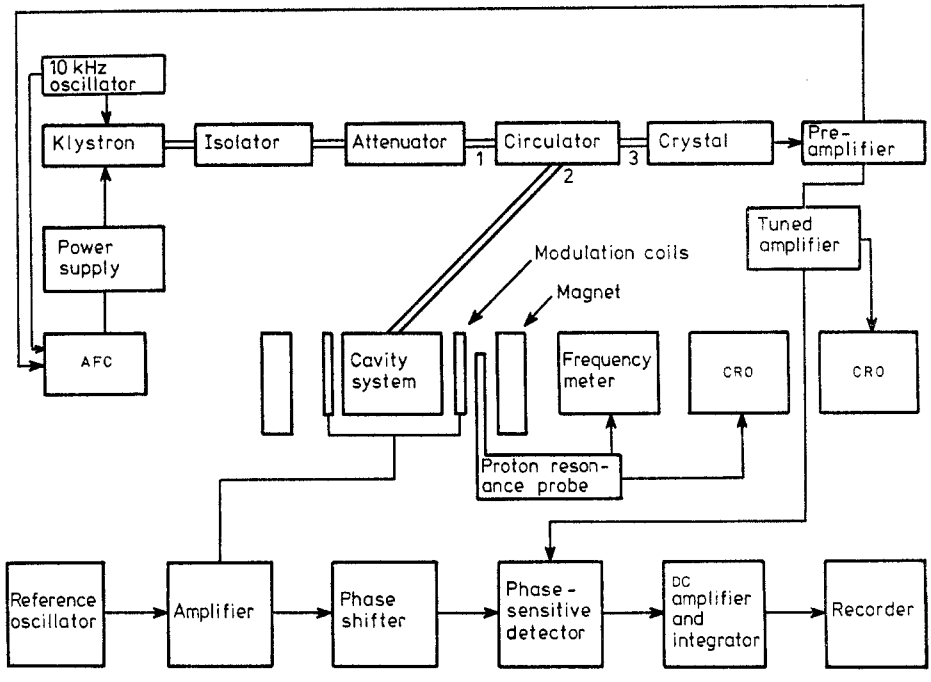

Figure 4. Block diagram of a typical field-modulated ESR spectrometer.

whose purpose is to increase the microwave magnetic field at the sample. It is easy to show that the impedance of the cavity at resonance is given by

$$Z_r = R(1 + 4\pi\eta Q\chi'') + i4\pi L_0\omega\eta\chi'$$

where χ' and χ'' are the real and complex parts of the susceptibility, Q is the quality factor of the cavity and η is the filling factor since not all the volume occupied by the cavity magnetic energy is filled with the sample. Since the resistive term determines the energy dissipation this expression shows directly the way in which the resonant structure augments by a factor Q the effect of χ''. This change in impedance at the magnetic resonance where χ'' goes through a maximum causes a change in the power reflected from the cavity and hence a change in the power transmitted along arm 3 of the circulator. This radiation is detected in a rectifier crystal and the signal appropriately amplified. Two forms of display are common. If the magnetic field is varied

at perhaps 50 Hz around the steady field value by an amount which is larger than the absorption linewidth then the output shows a dip whenever the resonance condition is reached. This may be displayed on an oscilloscope with a related time base. This system which requires a large bandwidth amplifier is inherently insensitive. The other method employs a small high-frequency (100 kHz) modulation while the large steady field is slowly swept through the magnetic resonance. If the modulation amplitude is much smaller than the linewidth a simple Taylor expansion shows that the component of the detector current at the modulation frequency which exists in the neighbourhood of the resonance will be proportional to the derivative of χ'' with respect to H. By beating this signal with a reference signal at the modulation frequency, a DC signal will be obtained proportional to $d\chi''/dH$. This signal can then be recorded on an X–Y recorder against H. This system accepts only the noise within a narrow bandwidth near the modulation frequency and if the line is traversed very slowly this method of phase-sensitive detection makes it possible to use bandwidths as small as $0{\cdot}1\ s^{-1}$. In figure 4 the further refinement of automatic frequency control is shown. The system shown there introduces a small modulation of the klystron reflector voltage at about 10 kHz. If the klystron drifts off the cavity resonance, there is a reflected signal at the modulation frequency. Precisely on cavity resonance the reflected signal at the frequency is zero. If the reflected signal is phase-sensitively detected an error signal is obtained which is applied to the klystron's reflector and will return it to the cavity resonance. Thus the detected signal will be strictly proportional to the derivative of χ'' and the dispersive part of the susceptibility will have no effect.

There are many other types of spectrographs, like the superheterodyne, monodyne systems, etc. References to the latest designs can be found in Poole (1967).

3. Resonance studies in diamond

While the form of the spin Hamiltonian is determined by symmetry a physical model must be used to estimate coefficients such as the g factor and the zero-field splitting parameters occurring therein. Ludwig and Woodbury (1962) in their excellent review of electron spin resonance in semiconductors remark that there are two basic models within whose framework most spin resonance systems in semiconductors can be treated. The first one, the crystalline field approach developed by Abragam and Pryce (1951), is appropriate only if the unpaired electrons are localised near the lattice site occupied by the impurity ion or lattice defect while the second model has the unpaired electrons so non-localised that their resonance properties are determined largely by the energy band structure of the host lattice. This second model usually applies in the case of unpaired electrons in a conduction band or bound to an impurity having a donor level shallow with respect to such a band. This model is not applicable to defects in diamond although it might have some applicability in the case of boron. The difference is due to the much larger energy gap of diamond and the tighter binding of the valence electrons in diamond. (In diamond only pure 2s and 2p orbitals are involved whereas in silicon and germanium the d orbitals are within easy reach of the valence electrons.)

3.1. Donor impurities

3.1.1. Dispersed substitutional nitrogen: the P1 centre. Smith *et al* (1959b) were the first

to observe paramagnetic resonance in natural diamond which could be unambiguously assigned to a definite impurity.

(*i*) *ESR spectrum and interpretation.* The spectrum observed by Smith *et al* is shown in figure 5. Since this initial paper, other papers have appeared dealing with this centre in more detail with respect to both experimental and theoretical aspects of this centre. Loubser and du Preez (1965) investigated the ^{13}C splitting as well as the forbidden quadrupole lines in the spectra in more detail, while Every and Schonland (1965) and Bower and Symons (1966) gave a more thorough theoretical treatment of the model of the centre suggested by Smith *et al.*

The results showed that the paramagnetic electron ($S=\frac{1}{2}$) interacts with ^{14}N ($I=1$) and also with ^{13}C ($I=\frac{1}{2}$) nuclei in positions a, b, c and d in figure 1. The relevant parameters are given in table 1. From the number of lines it can be deduced that the unpaired electron of the nitrogen can be situated on any one of the four C—N bonds, and the symmetry axis of the hyperfine interaction with the ^{14}N is parallel to any of the four $\langle 111 \rangle$ bond directions.

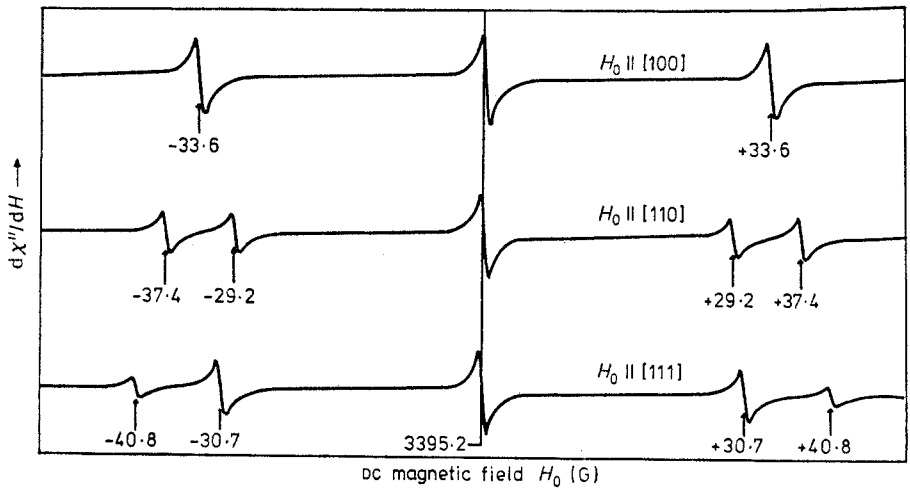

Figure 5. Derivative spectra of the P1 centre (after Smith *et al* 1959b).

Using the values of the hyperfine constants, and the theory outlined in §2.1, Bower and Symons (1966) deduced that for nitrogen $c_s^2=0{\cdot}06$ and $c_p^2=0{\cdot}23$ and for carbon in position (a) $c_s^2=0{\cdot}067$ and $c_p^2=0{\cdot}73$. The total spin population at the ^{14}N nucleus is therefore 0·29, whereas it is 0·79 on the unique nearest-neighbour carbon nucleus. This indicates then that the paramagnetic electron is localised almost entirely on the C—N bond and predominantly on the carbon atom. Smith *et al* proposed that this electron is accommodated in a C(sp^3)—N(sp^3) antibonding hybrid orbital. The p/s ratio for the nitrogen is seen to be 3·6 and for the unique carbon 10·9. Using Coulson's (1952) criterion for the variation of bond angle with the hybridisation ratio, this C—N bond on which the unpaired electron is situated is almost 10–14% longer than the usual C—N bond lengths. This distortion can be interpreted as a manifestation of the Jahn–Teller effect which states that if an orbital is degenerate it will distort to remove this degeneracy. Four independent antibonding orbitals are directed outwards from the nitrogen atom towards its four carbon neighbours. Placing the extra electron in one of these up to now degenerate orbitals will cause the orbital to distort

Table 1. Nitrogen centres in diamond. The hyperfine coupling constants of nitrogen and ^{13}C atoms, together with the p/s ratio of the wavefunction of the paramagnetic electron (constants in units of 10^{-4} cm^{-1}).

Centre†	g factor	A_1	A_2	A_3	θ (deg)‡	A_{iso}	A_{anis}	p/s	Reference
P1	2·0024 ± 0·0002	Nitrogen: 38·01 ± 0·01	27·12 ± 0·01	27·12 ± 0·01	35·3	30·76	3·63	3·8	Smith *et al* (1959b)
		(*a*) ^{13}C: 113·5	47·4	47·4	35·3	69·4	22	10·9	Cook and Whiffen (1966)
		(*b*) ^{13}C: 4·5							Loubser and du Preez (1965)
		(*c*) ^{13}C: 8·6							
		(*d*) ^{13}C: 14·1	10·7	10·7	35·3	11·7	1·17	3·3	
N1	2·0024	Nitrogen (1): 43·4 ± 0·5	29·9 ± 0·5	29·9 ± 0·5	35·3	34·4	4·50	4·20	Shcherbakova *et al* (1969)
		Nitrogen (2): 3·0 ± 0·3	2·7 ± 0·3	2·7 ± 0·3	35·3	2·8	0·1	1·16	
W7	2·0028 ± 0·0003	Nitrogen (1): 41·3 ± 0·3	29·2 ± 0·3	29·2 ± 0·3	35·3	33·19	3·93	3·87	Loubser and Wright (1973a)
		Nitrogen (2): 5·2 ± 0·3	4·4 ± 0·3	4·4 ± 0·3	144·8	4·67	0·27	1·88	
OK1	g_1 = 2·0019 ± 0·0003 g_2 = 2·0031 ± 0·0003 g_3 = 2·0025 ± 0·0003	7·164 ± 0·005	5·303 ± 0·005	5·293 ± 0·005	22·4 *A* tensor 45·2 *g* tensor	≃5·9	≃0·62	≃3·4	Klingsporn *et al* (1970)
N4	2·002 ± 0·001	Nitrogen (1): 30·5 ± 0·1	22·2 ± 0·1	22·2 ± 0·1	35·3				Welbourn and Woods (1977)
		Nitrogen (2): 29·9 ± 0·1	21·7 ± 0·1	21·7 ± 0·1		24·7	2·75	3·6	
P2	2·003 ± 0·001	3·67	3·37	3·37		3·47	0·10	0·94	Smith *et al* (1959a) Loubser and Wright (1973b)
N2	2·003 ± 0·001	ΔH = 2·4 G	—	—	—	—	—	—	Shcherbakova *et al* (1975)
W21	g_1 = 2·003 ± 0·002	Nitrogen (1) } : 6·8	4·1	4·1	—	5·0	0·9	5·84	van Wyk *et al* (1978)
	g_2 = 2·004 ± 0·002	Nitrogen (2) }							
	g_3 = 2·009 ± 0·002	Nitrogen (3): 38·7	≃0	≃0	—	12·97	12·87	32·1	
N3	2·003	1·7	0·5	0·5	29	0·9	0·4	14·4	Shcherbakova *et al* (1972)

† Models for centres are shown in figure 6.
‡ For orientation of A_1, A_2, A_3 and g_1, g_2, g_3 refer to figure 2.

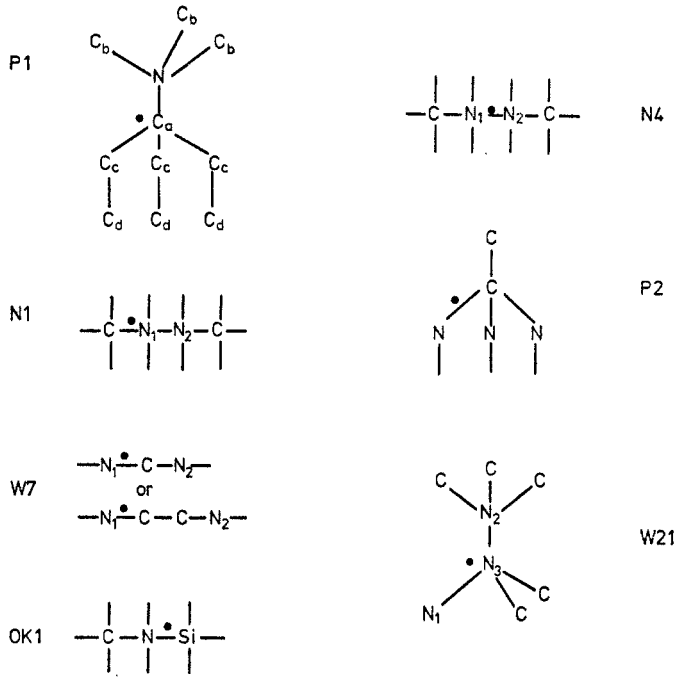

Figure 6. Diagrammatic models of some of the nitrogen centres in diamond.

in such a way that it has a lower energy than the other three. This extra unpaired electron is now caught in this one non-degenerate antibonding orbital and its contribution to the orbital magnetic moment is completely quenched, giving it a spin-only magnetic moment. Thus the g factor is isotropic and is close to the free-spin value, the small difference arising from spin–orbit coupling. At room temperature the centre thus shows a static trigonal Jahn–Teller distortion from T_d to C_{3v} symmetry.

These three sets of lines are all three times as intense as the set of lines due to the unique ^{13}C atom and they must therefore be due to ^{13}C atoms in three symmetrically equivalent carbon positions. The identification by Bower and Symons (1966) of the position of the carbon atoms giving rise to the second largest splitting as being in position C_d in figure 1 rests on the fact that the C_d—C_c bonds are parallel to the C_a—N bond, and that by some hyperconjugation mechanism some spin density is transferred to the C_d—C_c bond. The other lines are due to ^{13}C in positions C_c and C_b in figure 1. The accurate measurement of the intensity and positions of the ^{13}C satellites is therefore essential for the verification of any detailed theoretical model of a defect centre.

Loubser and du Preez (1965) also observed additional weak lines halfway between the sidelines and the centre line of the nitrogen spectrum. These they attributed to forbidden transitions $\Delta M = 1$, $\Delta m = \pm 1$ in the nitrogen spectrum which will occur due to the quadrupole coupling term mixing the different hyperfine levels (see Bleaney 1951). From the small observed splitting of these forbidden lines an estimate of $P = 3eqQ/4I(2I-1) = -5{\cdot}6$ MHz was made. In this expression Q is the quadrupole moment of nitrogen and q, the electric field gradient at the nitrogen nucleus, is given by:

$$q = -e \sum \langle (2z^2 - x^2 - y^2)/r^5 \rangle$$

where the sum is over the donor and eight bonding electrons. These matrix elements

were calculated by Every and Schonland (1965) and using the values obtained for the wavefunctions of the electrons a value of $Q = 0{\cdot}014 \times 10^{-24}$ cm^2 was found. The value of Q was reduced to $Q = 0{\cdot}01 \times 10^{-24}$ cm^2 using the more accurate value of $P = -3{\cdot}974 \pm 0{\cdot}001$ MHz obtained by Cook and Whiffen (1966) by means of the ENDOR technique. This is well within the range of other estimates of the quadrupole moment of nitrogen.

(*ii*) *ENDOR measurements.* Cook and Whiffen (1966) made extensive ENDOR measurements on the nitrogen centre. Apart from the very accurate determination of the quadrupole coupling coefficient they also observed a small change in the anisotropic hyperfine coupling with temperature, but not in the isotropic and the quadrupole coupling. This increase of the anisotropic coupling, which arises from dipole–dipole interaction, with a decrease in temperature is in order of magnitude agreement with the volume change, as one might expect, while the isotropic part which arises from a δ function will be less sensitive to changes in electron distribution away from the nucleus.

(*iii*) *The Jahn–Teller effect.* Sturge (1967) has given an excellent review of the role that the Jahn–Teller effect plays in solids. In the present treatment only the consequences of the effects in diamond will be discussed and then only in a qualitative way. With this in mind the Jahn–Teller theorem states that a non-linear molecule with a degenerate partially occupied orbital will distort to remove the degeneracy. In the case of a defect in a crystal lattice the presence of nearby impurities or external fields can also remove the degeneracy. It was argued in §3.1.1(*i*) that the nitrogen centre at room temperature exhibits a static trigonal Jahn–Teller distortion with no signs of reorientation. Shul'man *et al* (1967) observed reorientation of the nitrogen centre above room temperature with an activation energy of about 0·7 eV. Loubser and van Ryneveld (1967) measured a value of 0·76 eV. Similar dynamic Jahn–Teller reorientation effects have been observed by Watkins and Corbett (1964) in the vacancy-phosphorus centre in silicon but this occurred at 15 K. Reorientation of the nitrogen centre due to applied stress has not yet been reported.

(*iv*) *Relaxation and exchange interaction effects.* Loubser *et al* (1965) found very weak additional lines a third of the way between the main lines of the nitrogen spectrum of diamond coats. These they could explain as due to triads of nitrogen atoms with an antiferromagnetic coupling $J \simeq 2$ cm^{-1}. There were also two lines halfway between the three main lines which result when the magnetic field is parallel to the $\langle 100 \rangle$ direction. These two lines were not of the same intensity and are the forbidden $\Delta m = \pm 1$ lines due to the nuclear quadrupole coupling mixing the hyperfine states (Loubser and du Preez 1965). They also found that in cases of very heavily nitrogen-doped synthetic diamond powders the lines broadened and a single central line with small shoulders on the sides resulted. They could fit the experimental lines by using a Lorentz lineshape and averaging over all directions but one had to assume that the central line is 2·5 times stronger than the sidelines, i.e. exchange coupling was taking place.

Samsonenko (1965) observed that some natural diamonds had narrow nitrogen lines superimposed on top of very broad lines. The broad lines had a Gaussian shape in the wings but a Lorentzian shape in the centre and they argued that this shows that these lines are broadened by exchange interaction as well as by dipole–dipole interaction. From second moment calculations a figure for the most probable distance between magnetic centres of 21 Å was found. From geometrical considerations a value of $\sim 1 \times 10^{20}$ centres cm^{-3} was estimated while a similar technique for the narrow

lines gives a value of 3×10^{19} centres cm^{-3}. The volume having 10^{20} cm^{-3} concentration in some cases was estimated to comprise $\sim 2\%$ of the total crystal volume.

Faulkner *et al* (1965) investigated coated diamond and found one broad line of 40 G width, underlying the narrow nitrogen spectrum and assumed this line is due to exchange interaction between very closely spaced nitrogen centres. They give a figure of 5×10^{18} centres cm^{-3} for the narrower lines, which is about an order of magnitude less than Samsonenko (1965) claims for the concentration in a normal diamond.

Since then a number of papers have appeared by the Russian workers in this field using the techniques of second and fourth moment analyses of the very broad line observed in some diamonds containing nitrogen, as well as nitrogen lines in synthetic diamond powders. Shul'man and Podzyarei started with a paper in 1965, followed by papers in 1968 and 1972. Theoretical development of this type of analysis is based on van Vleck's (1948) original work. In their 1965 paper they find that there is definite evidence of clustering of nitrogen centres in synthetic diamond but in their 1972 paper they concluded that the impurities are basically randomly distributed in diamonds with a concentration up to 5×10^{19} centres cm^{-3}. At this point it is perhaps appropriate to remark that the major contribution to the linewidth in synthetic diamond is produced by the spread in the local field due to ferromagnetic inclusions (Dyer *et al* 1965).

Smith *et al* (1966) found that in synthetic diamond powders the concentration of the nitrogen centres is directly proportional to the reciprocal of the particle size and that the width of the central line decreases with a decrease in particle size. They argue that the reduction of the width of the central resonance is due to exchange narrowing because they estimate that in the core of each particle, in a sphere of 12 μm diameter, the concentration of centres has reached a value of 10^{20} cm^{-3}.

Zaritskii *et al* (1976) made an experimental and theoretical investigation of spin–lattice relaxation of nitrogen in two synthetic diamonds at temperatures of 4·2 K to 470 K and at various magnetic fields. They found $T_{1a}^{-1} = AT + BT^5$ and $T_{1b}^{-1} = CT + DT^4$ where the samples a and b had $N_a \simeq 8 \times 10^{17}$ centres cm^{-3} and $N_b \simeq 9 \times 10^{18}$ centres cm^{-3}. At $T = 4{\cdot}2$ K, values of T_{1a} and T_{1b} were independent of magnetic field in the range 400–4000 G. They considered the relaxation to be due to a phonon-induced tunnelling of the Jahn–Teller barrier accompanied by a reorientation of the electron spin because of the spin–orbit coupling and found good agreement with experiment.

(*v*) *Cross-relaxation effects.* A number of interesting relaxation effects has been observed which involves communication between two different species of spins within the same sample by means of spin–spin or dipole–dipole interaction. Bloembergen *et al* (1959) have called these processes cross-relaxation and called the time T_{21} which determines how fast two nearby resonances or spin systems are brought to the same effective temperature, the cross-relaxation time. The nitrogen spectrum in diamond with the magnetic field in the ⟨100⟩ direction consists of three equally spaced hyperfine lines and is ideal for investigating the simultaneous flip of four spins which exactly conserves Zeeman energy. The two spins of the centre line make a downward transition while a spin belonging to each satellite makes an upward transition. Using a bimodal cavity Sorokin *et al* (1960) pumped one hyperfine line with a saturating microwave pulse, and by monitoring the effect on another hyperfine line they could determine T_{21} which turned out to be of the order of 20×10^{-3} s, depending on the sample. This very elegant experiment also showed that in special cases the four spin flip transition could be used to establish continuous maser operation by inverting one of the satellite lines.

Cross-relaxation in synthetic diamonds was investigated by Shul'man and Podzyarei (1975) and will be discussed under nickel in diamond.

3.1.2. Other nitrogen centres.

(*i*) *The N1 centre.* This centre was observed by Shcherbakova *et al* (1969) in un-irradiated as well as irradiated and annealed natural diamonds. This centre appeared together with the P1 centre of the previous subsection. It has the same g factor with hyperfine constants which are about 10% larger than those of the nitrogen in the P1 centre but shows an additional splitting of each line into three equally intense lines. An analysis of the parameters and of the angular behaviour of this spectrum shows that the spectrum is due to the presence in the diamond lattice of two nitrogen atoms in neighbouring carbon positions, the unpaired electron being localised on one N—C antibonding orbital and interacting weakly with the second nitrogen atom. This model of a singly ionised nitrogen pair is supported by the fact that the hyperfine splitting due to the second nitrogen is in good agreement with calculation using the hyperfine splitting of the ^{13}C in the same geometrical position relative to the nitrogen atom in the N1 centre and noting that $A_{iso}{}^{C}/A_{iso}{}^{N} = 2{\cdot}0$. Shcherbakova *et al* suggest that these lines, which are often seen only in irradiated and annealed Ib specimens, are due to diamagnetic N—N centres already present in the diamonds, becoming partially ionised through electron capture by damage centres created during irradiation. In a later paper Shcherbakova *et al* (1972) propose that this centre is formed when a vacancy is trapped by the N—N pair to form a $(N_2V)^-$ centre.

(*ii*) *The W7 centre.* Loubser and Wright (1973a) found ESR spectra in brown diamonds at 77 K which were very similar to the N1 centre described above, differing in only two aspects. The spectrum only exhibits a maximum of six lines and not twelve lines, as was the case for the N1 centre, on either side of the centre line. The spectrum also changed as the temperature was raised above 200 K showing that averaging due to thermal reorientation was taking place.

Loubser and Wright suggested that the resonance was due to a singly ionised N_1—C—N_2 centre. At 77 K the electron is localised on the N_1—C bond and the hyperfine interaction with this nitrogen (N_1) shows axial symmetry about one of the $\langle 111 \rangle$ directions. The magnitude of the coupling constants is close to those measured for the P1 centre. A weaker interaction is observed with N_2 and it has axial symmetry about another $\langle 111 \rangle$ direction. The magnitude of the coupling constants for N_2 is about half of those due to a ^{13}C atom in the same position relative to the N—C bond as measured for the P1 centre. This seems to be consistent with the fact that:

$$A_{iso}{}^{C}/A_{iso}{}^{N} = 2{\cdot}0.$$

From the measurement of the broadening of the lines with increase of temperature when slow reorientation was taking place and the narrowing of the new lines that appeared at high temperatures, the activation energy of the dynamic Jahn–Teller effect was determined as $0{\cdot}24 \pm 0{\cdot}01$ eV by Loubser and Wright (1973a). It was clear from the spectrum that this N—C—N centre was not randomly distributed between all possible orientations but confined to sets of parallel {110} planes in the crystal.

Shcherbakova *et al* (1975) also observed this centre but postulated that this centre has an N_1CCN_2 structure close to the centre of a dislocation. They find that the N1 centre and the centre under discussion and another nitrogen centre (their ND centre) always occur in plastically deformed brown-coloured diamonds. They also attribute

the existence of a broad line at $g=2{\cdot}003$ as due partly to paramagnetic defects in the form of dislocations. It was shown earlier by Urusovskaya and Orlov (1964) that such brown diamonds show traces of plastic deformation and that similar colouring could be induced by plastically deforming diamond in the laboratory. Their idea of a translational slip by a distance equal to the Burgers vector $(1/\sqrt{2})\,a$ in the [110] direction, transferring the substitutional nitrogen pair N—N into a new centre N_1CCN_2, seems very plausible although the size of the hyperfine splitting of the second nitrogen and its $\langle 111\rangle$ symmetry around the C—N_2 bond is then difficult to understand.

(*iii*) *The P2 spectrum.* Smith *et al* (1959a) found a system of ESR lines in a great number of natural diamonds which usually have a pale yellow colour. This has since been called the '14 line' spectrum as they saw 14 lines when the spectrum presented its simplest appearance. They postulated it to be due to a substitutional aluminium atom but it was convincingly demonstrated by Every (1963) that this idea could not be correct. Since then Shcherbakova *et al* (1971) claimed that their calculation based on the model of a nitrogen–aluminium acceptor pair fitted the observed spectrum. Loubser and Wright (1973b), however, from their ENDOR measurements on this centre deduced that this centre is due to three equivalent nitrogens interacting with the same electron. They proposed that these nitrogens are substitutional and most probably in next nearest positions to each other. Their calculated ENDOR spectrum with $H\|\langle 100\rangle$ direction, assuming $\langle 111\rangle$ symmetry and using the values $A_\parallel = 11{\cdot}0$ MHz, $A_\perp = 10{\cdot}10$ MHz, $g_n = 0{\cdot}34$ and $P = -1{\cdot}0$ MHz, fitted the experimental spectrum quite well. Further measurements should, however, be done to elucidate the peculiar cross-relaxation effects observed in the ENDOR spectrum. They also illustrated that the Shcherbakova *et al* (1971) model does not fit the facts very well. Recently, van Wyk *et al* (1978) observed another centre in diamonds containing P2 centres, which also suggests interaction with three nitrogens. Two of these interactions are identical, and the third much larger. This centre is labelled W21 in table 1. The vexing question whether this '14 line' ESR spectrum or an underlying broad ESR spectrum correlates with the 4150 Å optical absorption spectrum will be discussed in a later section.

(*iv*) *The OK1 centre.* Klingsporn *et al* (1970) found a centre in a number of type Ib diamonds which had an anisotropic g, $S=\frac{1}{2}$ and was characterised by a small anisotropic hyperfine splitting exhibiting three closely spaced groups of lines. Klingsporn and co-workers showed that the hyperfine structure was due to nitrogen. The spin Hamiltonian parameters are given in table 1.

Shcherbakova *et al* (1972) confirmed the measurements of Klingsporn *et al* and suggested that this centre is a vacancy which has trapped a substitutional nitrogen to lower the symmetry from C_{3v} to C_{2h}. This model has, however, been proposed for another centre (W15) observed by Loubser and van Wyk (1977). The general features of the W15 centre are identical to those of the Si-G9 centre (Watkins 1967) where an aluminium impurity is trapped by a vacancy.

McNeil and Symons (1977) remeasured this centre and suggest that there is a substitutional oxygen atom next to a substitutional nitrogen atom. They argued that since the nitrogen hyperfine splitting is so small, the unpaired electron must be located near some atom that has no nuclear spin, like ^{16}O which has been found to be present in diamonds (Kaiser and Bond 1959). It could also be due to nitrogen plus a silicon which is also found in diamond.

(*v*) *The N3 centre.* Shcherbakova *et al* (1975) observed a system of lines very close to the central lines of the N1 and the OK1 centres. The spectrum was consistent with $S=\frac{1}{2}$ and $I=1$ and they attribute it to a nitrogen near a double vacancy.

(*vi*) *The N4 centre.* Shcherbakova *et al* (1975) also observed a spectrum which they ascribed to a $S=\frac{1}{2}$, $I=1$ system and which they called the ND centre. Welbourn and Woods (1977) showed that it was due to a $S=\frac{1}{2}$ system in which the electron couples to two almost identical nitrogens. (Shcherbakova *et al* observed only the outer lines of the spectrum.) The spectrum has ⟨111⟩ symmetry and Welbourn proposed that it is due to two substitutional nitrogens in nearest-neighbour positions sharing an electron. The p/s ratio of 3·6 is the same as that for the P1 centre.

This centre, like the W7 centre (Loubser and Wright 1973a), is not isotropically distributed throughout the crystal—only one of the four ⟨111⟩ directions being populated. The x-ray topographs of the sample showed that it had been plastically deformed, and it is possible that this N—N centre has been formed by plastic deformation. The {111} slip planes were predominant but it was not apparent that plastic deformation had occurred to a greater extent along any one set of parallel planes. This process was also suggested by Shcherbakova *et al* (1975) for the W7 centre.

3.2. Acceptor impurities

Spin resonance of shallow acceptor impurities in semiconductors are usually only seen in crystals subjected to uniaxial stress. The failure to detect the acceptor resonance in unstrained crystals is presumed to be related to the structure of the valence band.

The first reported ESR signal in diamond other than centres produced by irradiation with neutrons was observed by Smith *et al* (1959a). This is the P2 spectrum discussed under the nitrogen centres. As explained there they tentatively attributed this set of lines as being due to the acceptor aluminium but did not do any detailed theoretical analyses of the spectrum. It is now, however, clear that the spectrum is not due to aluminium but to an aggregate of three nitrogen atoms.

Bell and Leivo (1967) found a fairly broad line in natural semiconducting diamonds which they attribute to the acceptors in the natural semiconducting diamond. Since then it has been established that the acceptors must be boron (Collins and Williams 1971, Chrenko 1973).

Bourgoin *et al* (1972) found two broad lines in synthetic diamonds heavily doped with boron which appear to have a high level of grown-in strain. The widths of the lines vary with sample and were about 200 G wide. Both lines have an anisotropic g with a ⟨122⟩ axis of symmetry. The g values, as well as the intensity, depended very strongly on the temperature as well as the sample. The activation energy of the defect was determined from resistivity measurements and found to be 0·330 eV, the same as for the acceptor impurity in natural diamonds (Brophy 1955, Leivo and Smoluchowski 1955, Austin and Wolfe 1956, Wedepohl 1957, Lightowlers and Collins 1966, Williams *et al* 1970, Bezrukov *et al* 1970).

The widths of the lines did not change very much with temperature but one of the lines showed an amplitude variation close to an exponential law in $1/T$ corresponding to the same activation energy of 0·330 eV as determined from the resistivity measurements. The intensities of the lines were correlated, the one growing and the other decreasing in intensity when the sample was illuminated with white light. The influence of stress up to 12 000 kg cm^{-2} showed no shift in line positions but did increase the intensity of both lines. A natural semiconducting diamond was studied but no lines were seen. It was less conducting and Bourgoin *et al* argued that the lower boron content was responsible for the negative result.

The anisotropy (defined by $g_\perp/g_\parallel$) of the observed g values is about 5 which is greater than in silicon where Feher *et al* (1960) observed a g anisotropy of about 2 and only a small stress dependence of g. They interpreted their results in terms of a strain-induced splitting of the $J=\frac{3}{2}$ state into $M=\pm\frac{1}{2}$ and $M=\pm\frac{3}{2}$ doublets, the resonance transition taking place between $M=-\frac{1}{2}$ and $M=+\frac{1}{2}$ states. If the splitting of the $J=\frac{3}{2}$ ground state is sufficiently small J remains a good quantum number and one expects the spin Hamiltonian:

$$\mathscr{H}=g\beta \boldsymbol{H}.\boldsymbol{J}+DJ_z^2$$

to describe the spectra. It was shown by Ludwig and Woodbury (1962) that if $D\gg h\nu$ the anisotropy should be about 2. Bourgoin *et al* argued that in the case of boron in diamond the large anisotropy of g, and also the fact that it is strain-dependent, is due to the fact that the zero-field splitting is not large compared to $h\nu$. They postulate the one line as due to free holes in the valence band and the other one, which was enhanced by white light, as due to bound holes being excited as the light had only enough energy to induce valence-band to boron-level transitions.

The fact that in small diamonds which they were able to stress, an increase in the amplitude was observed rather than a shift is attributed to the external stress enlarging the volume of the crystal experiencing the predominantly grown-in stress. They did not observe the sharp line ($\Delta H\simeq 1$ G) observed by Bell and Leivo (1967) for natural semiconducting diamond which was attributed by them to acceptor centres, on the basis that the number of acceptors obtained by Hall and resistivity measurements was comparable to the number of spins measured in these natural stones by ESR.

3.3. Transition-metal ions

Most of the iron group and some of the 4d and 5d group ions have been observed in silicon. Also, impurity pairs consisting of transition-metal ion pairs as well as transition-metal ions paired with shallow ions have been extensively studied (Ludwig and Woodbury 1962). The presence of iron and nickel has been established by Sellschop *et al* (1974) in neutron activation studies. No resonance has thus far been reported for any of these ions in natural diamonds.

In synthetic diamond the only reported transition-metal ions that seem to be responsible for ESR spectra are iron, nickel and cobalt. The identification of the observed spectra, as actually being due to isolated iron ions and to substitutional nickel or cobalt, is by no means unambiguous.

3.3.1. Ferromagnetic aggregates and dispersions. Huggins and Cannon (1962) detected very broad lines in synthetic diamond made with various metals as catalyst, and also in diamonds that were prepared by high-pressure, high-temperature diffusion of the doping element into existing synthetic diamonds, both in the absence and presence of a transition-metal catalyst. In all cases except boron-doped diamond, the characteristic three lines due to nitrogen were observed on the synthetic diamond grit. In all of the diamonds except those using aluminium as a catalyst a broad line was seen which they claimed was characteristic of transition-metal impurities in dispersed form. The width of nitrogen lines in the synthetic powders was proved to be due to the ferromagnetic impurities by Dyer *et al* (1965). They investigated diamonds grown from a non-ferromagnetic catalyst, Brightray-S, and found that the linewidths were reduced from 8 G to about 4 G.

Smith and Angel (1967) found that on heating diamond grit to 1500 °C for 15 s in vacuum the linewidths were reduced to 3 G. The broad lines also disappeared after heating but some samples were still attracted by a magnet. These stones also exhibited an additional broad line at a slightly lower g than the nitrogen and Smith and Angel speculated that this line might be due to a free radical produced by carbonisation very near the surface, but not to graphite. They also analysed the residue of these diamonds after oxidising by air and found nickel and iron in them. The g factor of the broad ferromagnetic lines could not be determined by rotation of single crystals of synthetic diamond as the position of the lines in a fixed direction varied from sample to sample. It therefore seems unlikely that the ferromagnetic inclusions have a preferential shape or lie in any particular plane. The effect of the heating is ascribed to the melting of larger aggregates of metal inclusions which exert pressure on the diamond so that a distribution of cracks is produced along {111} cleavage planes through which the additive metal escapes. Some of the additive metal catalyst, however, exists in a finely dispersed form which has quite different properties.

3.3.2. Nickel: the W8 centre. In addition to the broad lines due to gross ferromagnetic inclusions in diamond and the nitrogen triplet observed in synthetic diamond powders, another line with $g = 2{\cdot}0310 + 0{\cdot}0005$ was observed by Loubser and van Ryneveld (1966) at temperatures below 250 K. The intensity of this line relative to the intensity of the nitrogen was sample-dependent as was its width—about 6 G. They ascribed it to nickel, as diamonds grown from an iron melt with very little nickel showed a line of much reduced intensity whereas diamonds grown from a cobalt melt showed no such line. Subsequently Loubser (1977) found this centre, W8, also in finely powdered (particle size 0·5–30 μm) natural diamonds. It was shown that the centres which give rise to this line were present a fraction of a micron below the surface. The diamonds were powdered in a metal ball mill. The balls, however, did not contain any nickel. It is thus unlikely that nickel could have diffused into the diamond on grinding and this line must be due to some other defect. Podzyarei and Zaritskii (1968) attributed this line to a centre consisting of a substitutional nitrogen plus oxygen and observed a Jahn–Teller distortion below 4 K while Loubser and van Ryneveld (1966) saw no change at 4 K. Bratashevskii *et al* (1972) think it is due to an interstitial carbon but no such centre has been seen in single crystals of irradiated diamond or in irradiated and annealed diamond. Shul'man and Podzyarei (1975) made relaxation measurements on synthetic diamonds containing this W8 centre as they had observed that the P2 nitrogen centre's sidelines were much stronger on the low-field side where the single line of the W8 centre overlapped these sidelines. Due to cross-relaxation the low-field sidelines of the P2 centre were de-saturated and appeared stronger than the central line and high-field sidelines. The measured relaxation time of the central nitrogen line was found to be $\tau_{N2} = 10^{-3}$ s at 77 K while that of the W8 centre is given by $\tau_{W8} = 2 \times 10^{-4}$ s.

3.3.3. Cobalt. Bagdasaryan *et al* (1975) investigated diamonds synthesised at pressures of 45 kbar, and temperatures of 1100 °C using graphites of various types and pure metals such as Fe, Ni, Cr, Mn and Co and their mixtures. The high-pressure capsule was made of tungsten carbide containing 6% Co. They found that, in addition to the nitrogen P1 ESR system and the W8 ESR system of lines, all investigated samples gave an ESR signal at 77 K in the region of $g \simeq 4$. From the powder ESR signal they deduced that $g_{\parallel} = 4{\cdot}117 + 0{\cdot}005$ and $g_{\perp} = 4{\cdot}43 + 0{\cdot}03$. They also claim that a hyperfine structure

corresponding to the $I=7/2$ of the Co nucleus is discernible on the wide line. The measured values of the hyperfine constants are $A_{\parallel}=(245\pm 8)$ MHz and $A_{\perp}\simeq 260$ MHz. At room temperature this powder line is very broad. They measure the concentration as $2\text{–}3\times 10^{16}$ ions g^{-1}. The intensity of the ESR lines was almost doubled in diamonds synthesised by means of a cobalt-containing catalyst (8% Co). They speculate that the Co^{2+} ions are located on the almost octahedral interstitial sites of the diamond lattice where the four nearest-neighbour atoms are tetrahedral and the six next-nearest neighbours are octahedral, but as the octahedral crystal field is larger they argued that the tetrahedral field can be neglected. Co^{2+} therefore gives a ground state as an orbital triplet T_1 state. Spin–orbit interaction then splits the T_1 level into a doublet, quartet and a sextet. As shown by Abragam and Bleaney (1970) the main term giving paramagnetic resonance is the doublet with an isotropic g factor of 4·33 which coincides with the average of the g factor of the cobalt in diamond. This agreement with theory seems to indicate that there is no quenching of the orbital angular momentum due to covalent bonding and that the upper excited states are mixed with the ground state. The small anisotropy of the g factor they attribute to a slight tetragonal or trigonal distortion of the octahedral field.

An experiment using single crystals of synthetic diamond should be done to make the assignment of cobalt to this line unambiguous.

4. Irradiation damage centres

4.1. Introduction

A small concentration of point defects may drastically modify the electrical or optical properties of a material, quite often making the material useful in practical applications. Academic interest in defects has also been keen for many decades. A point defect is closely surrounded by neighbouring atoms and the defect problem is a many-body problem. It consists of the identification of the defect, an understanding of how the defect is introduced and removed, and an understanding of the changes in the physical properties of the material due to the presence of the defects. The experimentalist tries to identify and determine the nature of the defect. The construction of a 'simple' theoretical model that describes the observed properties is a challenge to the theorist.

The most common techniques by which defects are introduced in semiconductors are by irradiation with electrons, neutrons or heavy charged particles, or by plastic deformation. The results obtained are quite often different and usually complement each other. As this is not a review on defect production, only a brief explanation of the mechanism involved will be given. For more details see the reviews by Corbett (1966), Mitchell (1965) and Corbett and Bourgoin (1975).

The effect of the incident high-energy particle is to displace an atom from its normal lattice position to produce a vacancy and an interstitial. In the case of electron or heavy charged particle irradiation, the Coulomb potential around the nucleus governs the dynamics of the particle–nucleus collision. For neutron irradiation, the short-range nuclear forces are involved, and in the case of gamma rays, the Compton electrons produced by the gamma rays interact with the nucleus, and if of high enough energy could displace the atom concerned.

A great deal of energy can be transferred to the nucleus, but the average energy is considerably lower than the maximum, particularly in the case of the Coulomb

interactions. The long-range Coulomb interaction emphasises the low-energy interactions, while for neutrons, since its interaction cross section is almost isotropic, we get a much higher mean energy transmitted.

The recoiling atom interacts with its neighbouring atoms and various attempts have been made to calculate this interaction energy. If the energy of the primary recoil atom is low, the only result is a local heating of the lattice. Ultimately an energy will be reached where the recoil atom will be displaced to an interstitial site leaving a vacancy behind.

Because of the large recoil energies of the carbon atoms during neutron irradiation, the amount and pattern of damage is not readily calculable. If electrons of energy 1 MeV or less are used, the displaced atoms will not have sufficient energy to produce secondary damage. So by choosing the energy between 0·5–0·8 MeV only single vacancies will result (Mitchell 1965).

The single interstitial and vacancy can form close pairs or they can migrate in the form of free interstitials and vacancies. These free interstitials and vacancies may aggregate to form di-interstitials and di-vacancies, or they can interact with impurities and other defects to form complex configurations. The primary concern of irradiation studies is with the simpler systems but the experimental conditions are often such that complicated defects are invariably formed, and the study of these often gives evidence about simpler defects. This is indeed the case in irradiation studies in diamond, which cannot be obtained in as pure a state as, for instance, silicon.

It is now generally accepted that the impurities in diamond play a dominant role in determining the type of defect formed during irradiation, and during annealing after irradiation.

The study of irradiation damage centres in silicon has given us a real insight into the damage process and annealing behaviour of these centres (Watkins 1975). In the case of diamond much is still to be done and quite a number of the defect models presented are still very tentative, as well as the interpretation of annealing processes. We shall first discuss the centres produced in type IIa diamonds since these are the purest. Then type Ib will be discussed where, in addition to the centres observed in other types, many more centres are observed.

Before going into the details of the various observed centres let us look at some of the theoretical predictions of the properties of the neutral vacancy and the charged vacancy, as well as the state of the interstitial carbon.

4.2. Summary of the theoretical properties of vacancies and interstitials

The effective mass treatment of Kohn and Luttinger (1955) has been highly successful in describing the electronic structure of shallow impurity states in semiconductors. However, for deep levels ($>0{\cdot}01$ eV from the band edges) which represents a large number of the impurity states in covalent solids and practically all defect states produced by irradiation in these materials, no successful general theoretical description has yet been devised. Part of the problem is the importance of lattice relaxation and distortion around the defect or impurity, which is absent in the shallow states.

4.2.1. The defect molecule. A vacancy consists of an empty lattice site with the lobe of an sp^3 hybrid orbital pointing towards it from each of the four neighbouring carbon atoms. These orbitals which naturally have T_d symmetry were originally bonded to a

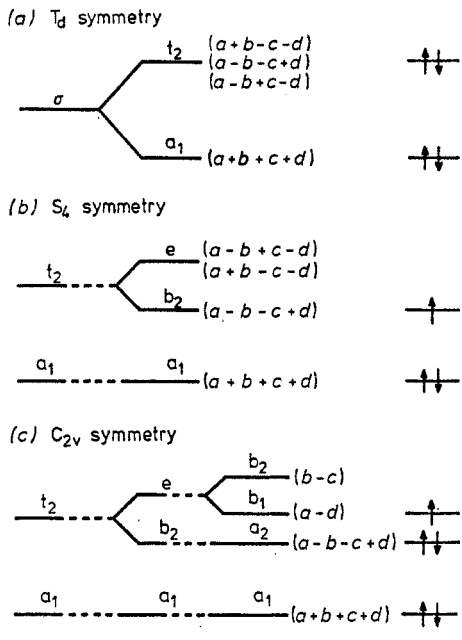

Figure 7. (*a*) Splitting of the bonding orbitals in cubic symmetry by overlap. On the right is shown how these orbitals are filled in the case of the neutral vacancy. (*b*) Splitting of the bonding orbitals as the symmetry is reduced from T_d to S_4 symmetry (tetragonal distortion) due to a Jahn–Teller distortion in the case of the positively charged vacancy. (*c*) The negatively charged vacancy has three electrons in the t_2 orbitals and partially occupy the e orbital of D_{2d} due to tetragonal distortion. The centre then undergoes a further trigonal distortion to C_{2v} symmetry. Note that only two orbitals *a* and *d* now appear in the zeroth-order wavefunctions as also observed in the hyperfine structure.

carbon atom occupying the site. The theoretical problem posed by this model was first tackled by Coulson and Kearsley (1957). They assumed that positively charged, neutral and negatively charged vacancies are formed when three, four or five electrons are accommodated in these orbitals.

Overlap between the orbitals will split the four-fold degenerate state as indicated in figure 7, where *a*, *b*, *c* and *d* are the wavefunctions representing the four dangling bonds. This gives the basic one-electron scheme of the defect (Watkins 1965). If the electrostatic and exchange interactions between electrons are neglected we can add successive electrons to the defect, filling up the levels as indicated in figure 7 which shows the neutral vacancy V, positively charged vacancy V^+ and the negatively charged vacancy V^-. When a degenerate orbital is partially occupied, the Jahn–Teller effect manifests itself and the defect will in general distort to remove the degeneracy. The presence of an impurity in an adjacent site, external electric fields or uniaxial stress can also remove the degeneracy. The positively charged vacancy will give a $^2T_2$ state which is unstable against a trigonal or tetragonal distortion and will distort to a S_4 symmetry.

This model has been put on a more quantitative basis for diamond by Coulson and Kearsley (1957), Yamaguchi (1962, 1963) and Larkins (1971a, b), who included electrostatic interaction between the electrons. They find that besides the low-lying states of minimum spin predicted by the one-electron theory, there are other low-

lying states of maximum spin. The relative positions of these states depend rather critically on the details of the calculation. However, in the case of silicon Watkins and Corbett (1961, 1964, 1965) and Watkins (1962, 1965, 1967) found that the ground state is always predicted by the simple model, although in one or two cases an excited state of higher spin has also been found. In particular, whenever orbital degeneracy is predicted by the one-electron model, Jahn–Teller distortion is seen in spin resonance.

The ESR study of defects in silicon by Watkins and Corbett (1965) and Watkins (1965, 1967) not only gave the symmetry of the defect but also gave a measure of the unpaired spin density on the various nuclei surrounding the defect through the hyperfine structure of the ^{29}Si which has a nuclear spin of $\frac{1}{2}$, and is 4·5% abundant. In diamond, however, the lines unfortunately have much weaker satellites due to the presence of the only 1·1% abundant ^{13}C which also has a nuclear spin of $\frac{1}{2}$.

The neutral vacancy shown in figure 7(*a*) with an electronic configuration $a_1^2t_1^2$ has a ^{1}E ground state in the one-electron model and no spin resonance is therefore predicted.

The negatively charged vacancy has three electrons in the t_2 orbitals and its Hund's rule ground state is $^4A_2$, which is also the ground state predicted by Yamaguchi's calculation (1963). The one-electron picture predicts that the lowest doublet of t_2^3 is an ^{2}E state which will show a Jahn–Teller splitting and might produce a level lower than the $^4A_2$. This is confirmed in the case of silicon. Watkins (1965) found a spin doublet ground state with C_{2v} symmetry as shown in figure 7(*c*).

The one-electron model also predicts the correct ground states for the (aluminium + vacancy)$^-$ complex and the (vacancy + phosphorus)$^+$ centres in silicon. The findings of the molecular orbital calculations for diamond, however, show that:

(i) An ESR absorption from an excited state $^3T_1$ with symmetry axis along ⟨100⟩ may be due to a V^0 or C^0 (C ≡ carbon interstitial).

(ii) A ground state with $S=\frac{3}{2}$ or $\frac{1}{2}$ may arise from a V^-.

(iii) A ground state $S=\frac{1}{2}$ may arise from C^-.

According to the theoretical predictions centres such as V^+ and C^+ are unstable. Very few of these predictions seem to hold for silicon and diamond. No defects have yet been identified with silicon interstitials in silicon or with carbon interstitials in diamond. As is so often the case the detailed molecular orbital calculations, such as those performed by Coulson and Kearsley, for example, turn out to be less successful than the naive version where the exchange and Coulomb interactions between valence electrons are neglected. These interactions, as Friedel *et al* (1967) point out, are probably quite large but the large configuration interactions tend to favour a low-spin rather than a high-spin ground state. Hagston (1970), however, suggests that the qualitative success of Watkins' models lies in the large electron–lattice interaction, i.e. the large Jahn–Teller effect. His calculations have, however, been criticised (Stoneham 1971).

Coulson and Larkins (1969) also calculated the electronic structure of the neutral isolated di-vacancy in diamond. They predicted a $^3A_{2g}$ ground state and predicted two strong optical transitions $^3A_{2g} \rightarrow {}^3A_{1u}$ and $^3A_{2g} \rightarrow {}^3E_u$. This centre should show an ESR transition.

4.2.2. Cluster calculations. Messmer and Watkins (1970, 1973a, b) and Watkins and Messmer (1970) were the first to calculate deep defect levels in semiconductors by simulating the real crystal by a large cluster of host atoms surrounding the defect, as suggested by Hoffman (1963). The electronic states of the entire system can then

be computed by linear construction of atomic-orbital–molecular-orbital techniques. They used the extended Hückel theory and clusters as large as 70 atoms. The calculations were first done for boron (Messmer and Watkins 1970), a substitutional nitrogen and the neutral vacancy (Watkins and Messmer 1970). The agreement between theory and experiment for the substitutional nitrogen was found to be good and for the vacancy experimental results on silicon showed good agreement in that a localised level of t_2 symmetry is produced in the forbidden gap when the central atom is removed. The level was found to be close to the valence-band edge with the wavefunction primarily localised on the four carbon atoms nearest the vacancy.

Larkins (1971a, b) has made a critical examination of the extended Hückel cluster calculations and comes to the conclusion that the results for point defects in diamond-type crystals should be considered to be only semi-qualitative. Weigel *et al* (1973) and Weigel and Corbett (1976) have made similar calculations of the interstitial carbon in the diamond lattice and the Jahn–Teller distortions for such an interstitial. They come to the conclusion that the carbon $\langle 100 \rangle$ split interstitial and bond-centred interstitials are the most stable with the split interstitial being the lowest in energy. This is contrary to the usual assumption that the most symmetrical sites correspond to lowest energies.

The only centre that has unambiguously been identified is the uncharged vacancy V^0, which gives rise to the optical GR1 band at 741 nm (Clark and Walker 1973, Walker *et al* 1974). Recently Douglas and Runciman's (1977) magnetic circular dichroism measurements on the GR1 line also confirmed that this line arises from a $^1E \rightarrow {}^1T_2$ transition at a neutral vacancy as predicted by the one-electron 'dangling' bond model. This centre is not paramagnetic and no ESR will be observed.

4.3. Radiation defects in irradiated type II diamonds

The measured values of the constants in the spin Hamiltonian, the symmetry and other properties such as growth rates and annealing behaviour will be discussed first. Possible models and origin of the zero-field splitting will then be dealt with.

The initial experiments were done by Griffiths *et al* (1955) and the first systematic detailed studies were carried out by Faulkner and Lomer (1962). A typical spectrum is shown in figure 8. The spectra which they observed were very complex and some space will be devoted to a discussion of the various systems identified by these and other workers.

4.3.1. Centres with lines close to $g = 2$. Any $S = \frac{1}{2}$ centre with no hyperfine interaction or g shift will give rise to a single isotropic line with $g = 2$. The isotropic line of width $\simeq$ 5 G, originally called the 'a' line, observed in all irradiated diamonds, could be due to any number of $S = \frac{1}{2}$ centres. A similar line appears to be present in all type IIa diamonds before irradiation and its intensity grows upon irradiation (Duncan 1965). Whether this line is the same as the 'C' line of width 2·4 G reported by Baldwin (1963) is not certain. Another isotropic line at $g = 2$ with weak side structure at ± 60 G and an even weaker satellite pair at ± 30 G was observed by Lomer and Wild (1971) after irradiation at 17 K and by Brosious *et al* (1977) after irradiation at 80 K. The ± 60 G spectrum does not seem to be associated with the same centre as the ± 30 G structure even if allowance is made for the possibility of charge effects. The side structures of ± 30 G only appeared after annealing to 150 K and disappeared at 220 K while the ± 60 G structure also appeared after irradiation at 80 K. Brosious *et al*

Figure 8. The ESR spectrum of irradiated diamond showing the R1 and R2 systems. The narrow lines are due to the R1 system and the broad ones to the R2 system. The central unresolved set of lines are due to the R3 and R4 (W6) systems. The field is parallel to the z axis of the R1 system (⟨994⟩) and the separation between the peaks is 3000 G.

(1977) found that it annealed out at 140 K. Lomer and Wild (1971) found it to grow on warming to 105 K. It is clear, however, that a substantial part of the central isotropic part has nothing to do with the side structures as after irradiation there was a 20% enhancement of the $g=2$ line already present in the sample and then a second enhancement after warming to 130 K. These enhancements disappeared after warming to 300 K. After irradiations at 80 K with larger doses of electrons Welbourn (1976) found that some of the isotropic $g=2$ line remains at 300 K which he suggests is the same $g=2$ isotropic line (the 'a' line) seen after room-temperature irradiation. Clark and Mitchell (1977) interpret these spectra as being due to one of two causes:

(i) A primary defect produced at 17 K but not in a magnetic state until 80 K, although produced directly in a magnetic state at 80 K.

(ii) A primary defect produced at 17 K but not forming a magnetic defect until it moves at about 80 K and becomes trapped at an impurity from which it is released at 275 K. It is possible that the defect is a Frenkel close pair or that it is some form of interstitial which is stable up to 250–300 K. This primary defect must be formed in addition to the vacancies, which give rise to the GR optical absorption, and the mobile interstitials (Welbourn 1976) which have migrated to impurities at 80 K (see discussion of R4 (W6)).

Baldwin (1963) claims that his A line is due to the charged state of the vacancy; hence this is a very important centre. He found that intensity of the A line was enhanced by illuminating the diamond with light with an energy larger than 2·8 eV and quenched by light of energy less than 1·1 eV. The A spectrum, which we will now call S1, is shown in figure 9. The field is parallel to ⟨110⟩ in this figure. The effect of the ultraviolet and red light on the S1 centre and its satellites which Baldwin

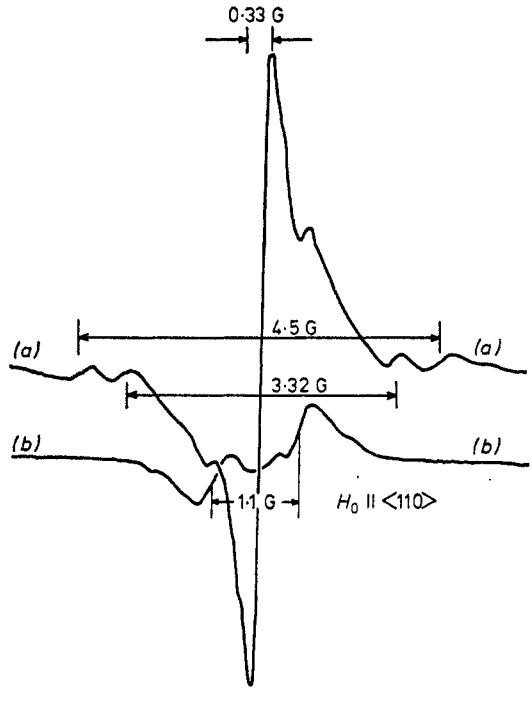

Figure 9. The Baldwin S1 and S2 system in irradiated diamond. (*a*) The spectrum with ultraviolet light illuminating the diamond—the S1 central line and two satellites shown on each side. (*b*) The spectrum with red light illuminating the diamond—S4 (or B) system.

attributes to ^{13}C nuclei is clearly visible. The 'B' centre (labelled S4 in table 2) mentioned by Baldwin (1963) is seen to be composed of two lines separated by about 1·1 G. When the phase of the 100 Hz field modulation is changed by 90° another line which he called 'C' becomes visible. Baldwin also observed another set of lines shown in figure 10 about halfway between the outer nitrogen lines and the centre line. He assumed that these are also ^{13}C satellites of the S1 centre. They, as well as the inner

Table 2. The Baldwin centres.

Centre	Proposed model	Hyperfine constants (10^{-4} cm^{-1})	Symmetry axis, *g* value and linewidth	p/s ratio
S1 (part of A centre)	[Vacancy]$^+$ with four nearest-neighbour carbons (for ^{13}C, $I=\frac{1}{2}$)	$A_\parallel = 4{\cdot}44$ $A_\perp = 3{\cdot}10$	⟨111⟩ $g = 2{\cdot}0023$ $\Delta H = 0{\cdot}4$ G	4·3
S2 (part of A centre)	Substitutional nitrogen ($I=1$) + some other defect	$A_\parallel = 23{\cdot}59$ $A_\perp = 13{\cdot}63$	⟨111⟩ $g = 2{\cdot}0023$ $\Delta H = 0{\cdot}4$ G	6·4
S3 (C centre)	—	Single line	$g = 2{\cdot}00238 \pm 0{\cdot}0001$ $\Delta H = 2{\cdot}4$ G	—
S4 (B centre)	—	Two lines separated by about 1 G	$g = 2{\cdot}0023$ $\Delta H = 0{\cdot}4$ G	—

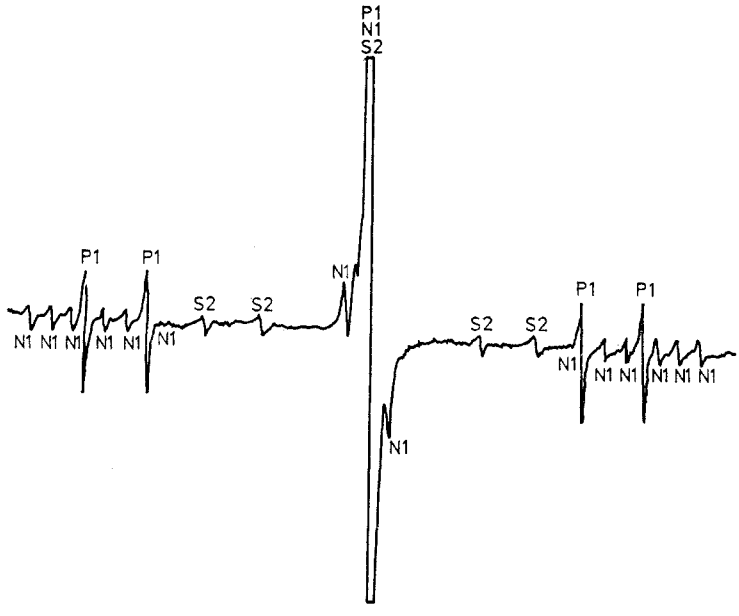

Figure 10. ESR spectrum of an electron irradiated (5×10^{-7} cm^{-2}) and annealed (400°C) type Ib diamond showing lines due to P1, N1 and S2 centres. The spectrum was taken at room temperature and the field range is 100 G.

satellites, have ⟨111⟩ symmetry. He therefore concluded that the S1 line was due to a carbon vacancy and that both sets of satellites are hyperfine components due to interaction of the paramagnetic electron in a t_2 orbital with ^{13}C nuclei. The inner and outer sets are associated with next-nearest and nearest neighbours respectively. However, measurements of the relative intensity of the two sets of satellites in three different irradiated diamonds showed large variations and did not give the theoretically expected ratio of 1:3 (Loubser 1975). This is fairly definite proof that the outer set of satellites does not belong to the 'a' centre. The outer set will now be called S2. Loubser suggested that this outer set of lines are hyperfine lines, not due to ^{13}C but due to nitrogen. The constants of the S1, S2 and S3 centres are given in table 2 where it is assumed that S2 is due to nitrogen.

Baldwin (1963) states that he used a type IIa diamond which showed a weak nitrogen signal due to the P2 centre. The S2 centre could therefore be due to some form of defect trapped at a nitrogen atom. The S1 centre could very well be a positively charged vacancy as Baldwin suggested, except that only a very small fraction of the electron's wavefunction is accounted for by assuming the hyperfine splitting is due to the four nearest-neighbour ^{13}C atoms. It is futile to speculate about the nature of the S1 and S2 centres on the few facts available.

4.3.2. S = 1 centres produced by irradiation at room temperature. The centres listed in table 3 seem to appear in both type IIa and IIb diamonds, after irradiation by electrons or neutrons.

The R1, R2, R3 and W6 (R4) centres have been studied most extensively by the Reading group and an excellent review has been written by Lomer and Welbourn (1977a). The two points that emerge from the study of the room-temperature ESR spectrum of irradiated IIa and IIb diamonds are firstly the complexity and secondly

the sample dependence of various parts of the spectrum. Both these facts suggest that impurities may be involved in many of the centres giving rise to this spectrum. In order that these centres are produced in the numbers actually observed by ESR, some component of the irradiation damage must migrate to the impurities at the irradiation

Table 3. Irradiation damage centres appearing in most diamonds irradiated at room temperature.

Centre	$\Delta g=(g-2)\times 10^3$ Major principal axis or θ and ϕ	$(D$† or A$)\times 10^4$ cm^{-1} Major principal axis or θ and ϕ‡	Linewidth (G)	References
R1	0 ± 4	$D_1=920$ $D_2=D_3=-460$ ⟨994⟩	5	Faulkner and Lomer (1962)
R2	0 ± 4	$D_1=920$ $D_2=D_3=-460$ ⟨100⟩	25–50	Faulkner and Lomer (1962)
R3	0 ± 4	$D_1=94$ $D_2=D_3=-47$ ⟨932⟩	5	Faulkner and Lomer (1962)
W6 (R4)	0 ± 4	$D_1=104\pm1$ $D_2=-69\pm1$ $D_3=-35\pm1$ ⟨111⟩	5	Lomer and Welbourn (1977a) Loubser (unpublished)
W4	0 ± 4	$D_1=49$ $D_2=D_3=-24{\cdot}5$ ⟨110⟩	5	Loubser (unpublished)
W5	0 ± 4	$D_1=35{\cdot}1$ $D_2=D_3=-17{\cdot}6$ ⟨110⟩	5	Loubser (unpublished)
A2	$\Delta g_1=1{\cdot}5\pm0{\cdot}5$ $\Delta g_2=3{\cdot}1\pm0{\cdot}5$ $\Delta g_3=3{\cdot}1\pm0{\cdot}5$ ⟨110⟩	$D_1=117{\cdot}5\pm0{\cdot}5$ $D_2=-60{\cdot}6\pm0{\cdot}5$ $D_3=-56{\cdot}6\pm0{\cdot}5$ ⟨110⟩		Kim *et al* (1973)
A3	1 ± 1 $\theta=30{\cdot}8$, $\phi=4{\cdot}5$	$D_1=-85{\cdot}8\pm0{\cdot}5$ $D_2=138{\cdot}9\pm0{\cdot}5$ $D_3=-53{\cdot}2\pm0{\cdot}5$ $\theta=30{\cdot}8$, $\phi=4{\cdot}5$		Kim *et al* (1973)
A1	$\Delta g_1=1{\cdot}6\pm0{\cdot}3$ $\Delta g_2=2{\cdot}1\pm0{\cdot}3$ $\Delta g_3=2{\cdot}6\pm0{\cdot}3$ $\theta=27$, $\phi=0$	$D_1=51\pm0{\cdot}5$ $D_2=-25\pm0{\cdot}5$ $D_3=-27\pm0{\cdot}5$ $\theta=8{\cdot}2$, $\phi=0$		Kim and Watkins (1971)

	^{13}C hyperfine interaction					
	A_1	A_2	A_3	θ	ϕ	Number of equivalent sites
I	9·7	12·7	9·7	0	53	2
II	6·8	8·8	6·6	0	45	2
III	5·2	7·2	4·8	0	41	2
IV	Average $A=3{\cdot}8$					4–6

† Major principal value is taken as positive.
‡ See figure 2.

temperature and be trapped by the impurities to give the observed ESR spectrum. As the vacancy is believed to be stable up to at least 700 °C it is proposed by Lomer and Welbourn (1977a) that a substantial part of the room-temperature spectrum is due to interstitial-impurity centres, different impurities giving rise to different systems. Besides carbon interstitial-impurity complexes being formed it is possible that the interstitial carbon atoms may change places with substitutional impurity atoms, forming impurity interstitials (cf group III interstitials in silicon (Watkins 1965)). In the case of the sample irradiated at 80 K (Welbourn 1976) only W6 and some unanalysed structure was observed immediately after irradiation and there was no change in the spectrum measured at 80 K, after annealing at room temperature. Thus, if interstitial carbon atoms are involved in the formation of W6, they must be mobile below 80 K. No information is available on the formation of R1, R2 and R3 at low temperatures. R1 has simply not been observed, R2 and R3 only become observable for measurement temperatures ~ 100 K as they are both due to paramagnetic excited states about 311 cm^{-1} above the ground state in case of R2 (Harris *et al* 1963) and 260 cm^{-1} in the case of R3 (Lomer and Welbourn 1977b). Whippey (1972) found no correlation between ESR intensity and dose for either the R1 or R2 centres. The R3 centre did not become visible until the dose had reached 3×10^{18} electrons cm^{-2} after which the intensity of the ESR lines grew fairly linearly with dose. The experimental intensity data can also be made to fit a $(\text{dose})^2$ dependence, in which case the data may suggest that the R3 centre is a di-vacancy.

The apparent difference in the conditions for the production of W6 and R4 (W6 was observed by Loubser directly after irradiation, while R4 appeared only after annealing to 500–600 °C (Whippey 1972)) can be explained by assuming that only a small fraction of the impurities which give rise to the R4 (W6) centre trap interstitials during irradiation. Further trapping occurs during annealing as mobile interstitials are released from other centres. This would explain the growth of the R4 system during annealing between 500 and 700 °C and R4 and W6 are indeed the same centre. Figure 11 shows the annealing of the GR1 optical band (now accepted to be due to a vacancy) and the ESR spectra in diamonds irradiated with 2·0 MeV electrons (after Clark *et al* 1964).

In figure 12 it can be seen that R1, R2 and R3 anneal out between 350 and 550 °C, whereas R4 anneals out between 800 and 900 °C. The disappearance of these centres at these temperatures may be due to the dissociation of the interstitial-impurity complexes, or to the annihilation of the interstitials by the mobile vacancies. The latter explanation looks attractive for R4 since it is believed that vacancies are mobile between 800 and 900 °C.

Owen (1965) discusses possible models for the R1 and R2 centres (then known as the C and B centres) extensively. In view of the later investigations of Lomer and Welbourn (1977a, b) which seem to prove that all these centres are interstitial-impurity centres, it may be necessary to revise these models and they will therefore not be discussed any further.

Kim and Watkins (1971) report the observation of another $S=1$ centre (labelled A1) in electron-irradiated diamonds. The major axis of symmetry is close to a $\langle 110 \rangle$ direction, and they suggest that it is due to either a four vacancy chain in the $\langle 110 \rangle$ direction of the $\{110\}$ planes or a split $\langle 100 \rangle$ interstitial and a vacancy with the same separation as this gives the correct value of $D = -\frac{3}{2} g^2 \beta^2 r^{-3}$ for two electrons situated on the dangling bonds at the end of the linear chain. This model has been successfully used to explain a number of ESR spectra found in irradiated silicon (Brower 1971), as

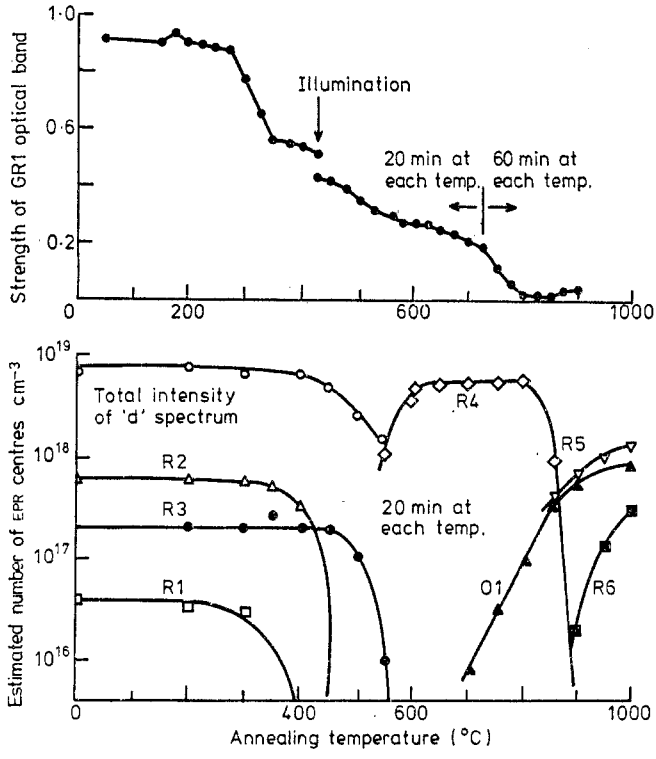

Figure 11. Isochronal annealing of the GR1 band and the ESR spectra in crystals irradiated with 2 MeV electrons. The break in the curve of the strength of GR1 at 425°C was the result of a single optical bleaching experiment using a high-pressure mercury lamp (after Clark *et al* 1964).

well as by Szendrei (1971) in his work on the W1, W2 and W3 centres found in unirradiated type Ib diamonds. The A1 centre, however, was formed by electron irradiation at room temperature, and it is hard to see how a four vacancy centre can be formed below the vacancy migration temperature. An interstitial-vacancy complex will most likely not be stable at room temperature as the interstitial is mobile at a much lower temperature (Lomer and Wild 1971).

Kim *et al* (1973) observed in addition two other $S=1$ centres (A2 and A3) in neutron-irradiated type I and II diamonds. The A2 centre has ⟨110⟩ symmetry, whereas the A3 is highly anisotropic with its major axis close to a ⟨112⟩ direction. They proposed that the former is due to a trivacancy formed in a {110} plane, while the latter is due to a vacancy pair situated along a ⟨112⟩ direction. The parameter values of these centres are given in table 3.

Several $S=1$ centres have been observed in natural diamonds, and it is thought that these centres are due to irradiation and possibly annealing during their geological history (Szendrei 1971). All of them have ⟨110⟩ symmetry except W10, which has ⟨111⟩ symmetry. W9 and W10 are almost identical to W4 and W6 respectively, where the latter are centres observed in type IIb diamonds. Parameters for these centres are listed in table 4.

4.3.3. Centres appearing after annealing at high temperatures. Lomer and Wild (1973) made a very thorough study of centres appearing in electron-irradiated type IIa

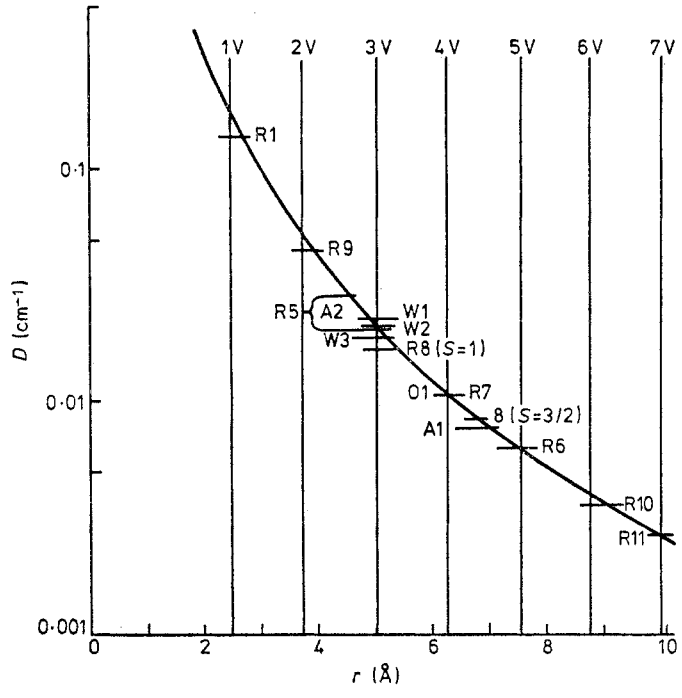

Figure 12. The variation of D with the separation of the components for a dipole–dipole interaction. The full curve is the theoretical curve calculated from equation (2.9). The experimental values are shown by horizontal lines (after Lomer and Wild 1973).

diamonds after annealing at various temperatures up to 1400 °C. Six sets of lines were identified following anneals in the temperature range 700–1000 °C. They all arose from centres with ⟨110⟩ symmetry and a spin of 1. The centres are thought to be formed by the trapping of mobile vacancies at impurities to give chains of vacancies of various lengths in the ⟨110⟩ direction of the $\{1\bar{1}0\}$ planes. Two further systems were observed after the 1100 °C anneal. At least one centre (R7) has a spin of $\frac{3}{2}$ and it seems

Table 4. Centres with $S=1$ occurring in natural diamonds.

Centre	Type of diamond	$D(\times 10^4\ \mathrm{cm}^{-1})$† and major principal axis	References
W1	Ib	$D_1=124{\cdot}7$, $D_2=-52{\cdot}35$, $D_3=-72{\cdot}35$ ⟨110⟩	Szendrei (1971)
W2	Ib	$D_1=137$, $D_2=-68{\cdot}5$, $D_3=-68{\cdot}5$ ⟨110⟩	Szendrei (1971)
W3	Ib	$D_1=153{\cdot}3$, $D_2=-76{\cdot}6$, $D_3=-76{\cdot}6$ ⟨110⟩	Szendrei (1971)
W9	IIA	$D_1=44$, $D_2=-22$, $D_3=-22$ ⟨110⟩	Unpublished
W10	IIA	$D_1=102{\cdot}7$, $D_2=-51{\cdot}4$, $D_3=-51{\cdot}4$ ⟨111⟩	Unpublished

† Major D value is taken positive.

likely that they were formed by some of the existing vacancy chains trapping an additional electron. Apart from an isotropic line with a free spin g value, all centres left after annealing to 1400 °C had ⟨111⟩ symmetry. Lomer and Wild suggest that at this temperature the vacancies may break away from the impurity traps and condense in rings such as a six vacancy loop on the {111} planes.

The eight centres found in annealed IIa diamonds with the temperature at which they are formed and anneal and the constants of the spin Hamiltonian are shown in table 5.

As pointed out it is most probable that the vacancy is involved in the formation of these ⟨110⟩ centres as the interstitials are already mobile at much lower temperatures. The various stages of annealing of the vacancy centre, which give rise to the GR1 optical absorption (see figure 11), suggest that the interstitial-impurity complexes which are responsible for the room-temperature ESR spectra are dissociating and the mobile interstitials will then start to anneal the GR1 centre.

The variation of D with the separation of the components of the dipole–dipole interaction calculated from the expression $D = -\frac{3}{2}g^2\beta^2 r^{-3}$ is shown in figure 12. As all the centres have exactly ⟨110⟩ symmetry and only odd-number vacancy chains can

Table 5. The characteristics of the ⟨110⟩ systems in annealed diamonds.

Centre	Annealing temperature (°C)	Spin	$D(\times 10^4\ \mathrm{cm}^{-1})$†	Linewidth (G)	Remarks
R5	850–1150	1	$D_1 = 190 \pm 2$ $D_2 = -88{\cdot}5 \pm 2$ } At 300 K $D_3 = 101{\cdot}5 \pm 2$ $D_1 = 140 \pm 2$ $D_2 = -63{\cdot}5 \pm 2$ } At 80 K $D_3 = -76{\cdot}5 \pm 2$	7 ± 2	Temperature-dependent D value
O1	700–1100	1	$D_1 = 70{\cdot}6 \pm 1$ $D_2 = -33{\cdot}4 \pm 1$ $D_3 = -37{\cdot}2 \pm 1$	$2{\cdot}2 \pm 0{\cdot}2$	Annealing associated with 1·18 eV optical centre
R6	800–1400	1	$D_1 = 41{\cdot}3 \pm 1$ $D_2 = -19{\cdot}7 \pm 1$ $D_3 = -21{\cdot}5 \pm 1$	$2{\cdot}0 \pm 0{\cdot}2$	
R7	1050–1400	$\frac{3}{2}$	$D_1 = 70 \pm 2$ $D_2 = -33{\cdot}1 \pm 2$ $D_3 = -36{\cdot}9 \pm 1$	$2{\cdot}7 \pm 0{\cdot}2$	
R8	1100–1300	1‡	$D_1 = 112 \pm 4$ $D_2 = D_3 = -56 \pm 4$	5	
R9	900–1250	1‡	$D_1 = 303 \pm 4$ $D_2 = D_3 = -151 \pm 4$	3	
R10	1000–1150	1‡	$D_1 = 23{\cdot}3 \pm 1$ $D_2 = D_3 = -11{\cdot}6 \pm 1$	2	Linewidth very small at low temperature
R11	900–1150	1‡	$D_1 = 18{\cdot}0 \pm 1$ $D_2 = D_3 = -9 \pm 1$	3	Linewidth very small at low temperature
R12	1100	1‡	$D_1 = 34{\cdot}6$ $D_2 = D_3 = -17{\cdot}3$		⟨111⟩ symmetry

† Major D value is taken positive.
‡ S could be $\frac{3}{2}$, in which case D values should be halved.

have exactly ⟨110⟩ symmetry it was suggested by Lomer and Wild (1973) that the centres R8, R9, R10 and R11 might have spins of $\frac{3}{2}$. It was very difficult to distinguish between $S=\frac{3}{2}$ and $S=1$ due to very strong central lines from other centres usually being present. They also found that the number of centres formed decreases as the number of vacancies in the chain increases. This would be expected if the chains increase in length by trapping further vacancies. They also found that the average number of vacancies per centre is about 3·8. This agrees with the observation that the concentration of the three and four vacancy centres is the highest.

Two centres, the R5 and A2 centres, have D values that are temperature-dependent. It cannot be due to thermal expansion otherwise D would decrease with temperature. Kim *et al* (1973) suggest that the lattice expansion is anisotropic and negative in the ⟨110⟩ directions but it is then impossible to explain why the same effect is not seen in all the ⟨110⟩ systems. Lomer and Wild (1973) used a model suggested by Dreybrodt (1967) for diatomic halogen centres in alkali halides. He argued that the average position of one of the atoms forming the centre may change as a result of the increasing amplitude of the thermal vibration in an asymmetric potential well.

4.4. Irradiation damage in type Ib diamonds

Apart from the centres R1, R2, R3 and A2, van Wyk and Loubser (1978) recently identified centres W11, W12, W13 and W14 in type Ib diamond that had been irradiated with 5×10^{18} neutrons cm^{-2}. Preliminary values of some of the parameters are given in table 6. All these centres have their major symmetry axis in a {110} plane

Table 6. Additional centres in neutron-irradiated type Ib diamonds (preliminary results).

Centre	D ($\times10^4$ cm^{-1})†, θ and ϕ	$(g-2)\times10^3$	References
W11	$D_1=291$, $D_2=$‡, $D_3=$‡ $\theta=44°$, $\phi\neq0$	0 ± 5	van Wyk and Loubser (1978)
W12	$D_1=318$, $D_2=$‡, $D_3=$‡ $\theta=37{\cdot}3°$, $\phi\neq0$	0 ± 5	van Wyk and Loubser (1978)
W13	$D_1=333$, $D_2=-129$, $D_3=-204$ $\theta=48{\cdot}3°$, $\phi=0$	0 ± 5	van Wyk and Loubser (1978)
W14	$D_1=361$, $D_2=$‡, $D_3=$‡ $\theta=35{\cdot}26°$, $\phi=0$	0 ± 5	van Wyk and Loubser (1978)

† Major D value is taken positive.
‡ To be determined.

close to a ⟨111⟩ direction. For two of the centres (W11 and W12) one of the minor principal axes is no longer perpendicular to a {110} plane ($\phi\neq0$ in figure 2). Here again, impurities trapped at various positions near the triplet centre probably give rise to the different symmetries of these centres.

Table 7 contains a list of centres found in irradiated and annealed type Ib diamonds. The centre W15 was found in neutron- and electron-irradiated Ib diamonds that had been annealed to about 600 °C (Loubser and van Wyk 1977). They then also exhibit a strong optical zero-phonon absorption peak at 638 nm together with associated phonon-assisted peaks spaced roughly 20 nm apart (du Preez 1965). Remeasuring the optical spectrum of this centre Davies and Hamer (1976) found that the zero-phonon

Table 7. Centres in irradiated Ib diamonds annealed at 600–900°C.

Centre	S	D ($\times 10^4$ cm^{-1}), θ and ϕ	Principal values of g tensor	Remarks
W15	1	$D_1 = 639$ $D_2 = -319{\cdot}5$ $D_3 = -319{\cdot}5$ $\theta = 35{\cdot}3°$ $\phi = 0°$	$g_1 = 2{\cdot}0028$ $g_2 = 2{\cdot}0028$ $g_3 = 2{\cdot}0028$ $\theta = 35{\cdot}3°$ $\phi = 0°$	Diamond annealed at 650°C
		^{13}C hyperfine constants		
		$A_1 = 68{\cdot}3$, $A_2 = 41{\cdot}1$, $A_3 = 41{\cdot}1$ $\theta = 141{\cdot}2$, $\phi = 0$ ($3{\cdot}5°$ from $\langle 1\bar{1}1 \rangle$) There are three equivalent sites.		
W16	1	$D_1 = 551$ $D_2 = -268$ $D_3 = -283$ $\theta = 37{\cdot}9°$ $\phi = 0°$	$g_1 = 2{\cdot}0029$ $g_2 = 2{\cdot}0026$ $g_3 = 2{\cdot}0022$ $\theta = 37{\cdot}9°$ $\phi = 0°$	Diamond annealed at 900°C
W17	1	$D_1 = 523$ $D_2 = -239$ $D_3 = -284$ $\theta = 38{\cdot}3°$ $\phi = 21{\cdot}6°$	$g_1 = 2{\cdot}0033$ $g_2 = 2{\cdot}0025$ $g_3 = 2{\cdot}0018$ $\theta = 38{\cdot}3°$ $\phi = 21{\cdot}6°$	Diamond annealed at 900°C
W18	1	$D_1 = 474$ $D_2 = -222$ $D_3 = -251$ $\theta = 38{\cdot}1°$ $\phi = 0°$	$g_1 = 2{\cdot}0033$ $g_2 = 2{\cdot}0027$ $g_3 = 2{\cdot}0023$ $\theta = 38{\cdot}1°$ $\phi = 0°$	Diamond annealed at 900°C
W19	1	$D_1 = 314$ $D_2 = -111$ $D_3 = -203$ $\theta = 20{\cdot}3°$ $\phi = 0°$	$g_1 = 2{\cdot}0028$ $g_2 = 2{\cdot}0031$ $g_3 = 2{\cdot}0029$ $\theta = 20{\cdot}3°$ $\phi = 0°$	Diamond annealed at 900°C
W20	$\frac{1}{2}$		$g_1 = 2{\cdot}074$ $g_2 = 2{\cdot}100$ $g_3 = 2{\cdot}018$ $\theta = 15°$ $\phi = 0°$	Only observed at 77 K after annealing at 400°C

line splits under pressure into components whose position, polarisation and intensities are predicted for a transition between an A_1 ground state to an E excited electronic state of trigonal symmetry. It is also known that vacancies start to become mobile at about this temperature and Davies and Hamer therefore suggested that this centre is a vacancy next to or near a substitutional nitrogen. This centre does not show an ESR spectrum but on illumination with light (Loubser and van Wyk 1977) a set of lines was observed with $S = 1$, $D = 960 \pm 2 \times 10^{-4}$ cm^{-1} with $\langle 111 \rangle$ symmetry.

The interesting thing about this centre is that the high-field lines were found to be in emission as shown in figure 13. With H parallel to the major principal axis each fine line is split into three hyperfine lines 0·8 G apart. The weak satellite lines seen on the outer two lines in figure 13 are due to ^{13}C hyperfine interaction (the splitting being 46 G in this direction), while a smaller interaction with another set of ^{13}C atoms

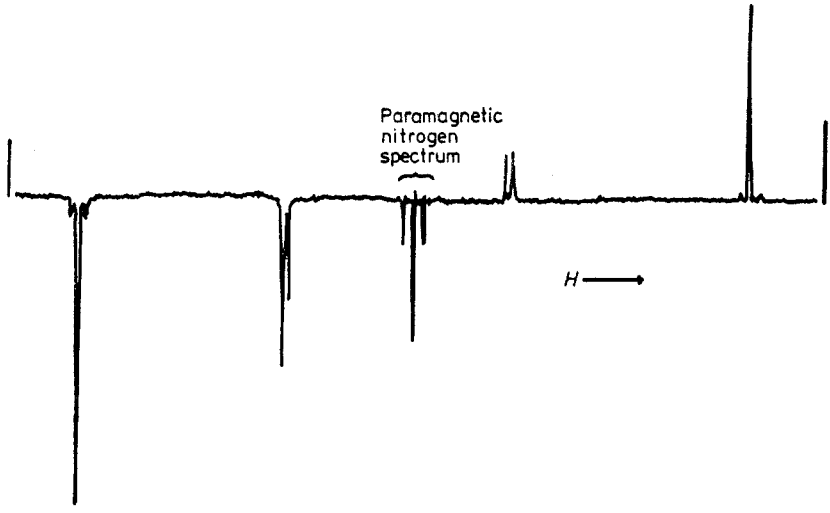

Figure 13. ESR spectrum of the W15 centre. The spectrum is shown in dispersion and the high-field lines are seen to be in emission if compared to lines of the P1 centre (in the middle of the spectrum). The weak lines close to the outermost lines are due to ^{13}C hyperfine interaction.

results in an isotropic splitting of 5·4 G. The intensity of both sets of satellites indicated that three equivalent carbon atom positions are involved. The angular dependence of these ^{13}C satellite pairs which appear on either side of all the fine-structure lines indicated an axial hyperfine interaction around three $\langle 111 \rangle$ axes, where these axes are not coincident with the principal D axis. In figure 14 the suggested model (Loubser and van Wyk 1977) is shown as well as the suggested one-electron orbitals.

The model of the vacancy next to a nitrogen atom seems to satisfy most of the

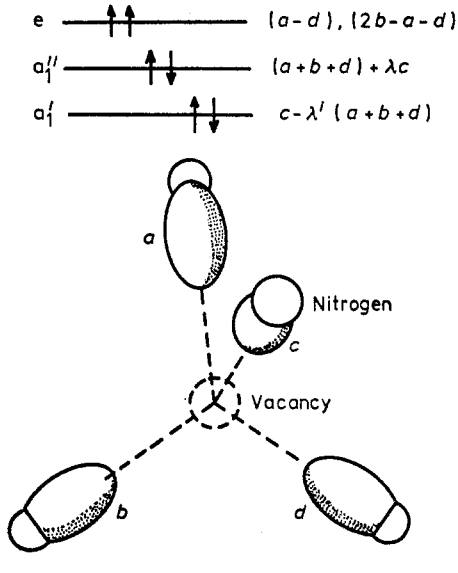

Figure 14. A possible energy-level scheme and simple LCAO one-electron molecular orbitals for the nitrogen-vacancy pair in the excited triplet state $^3A_2$.

observed facts if it is assumed that the centre has captured another electron. The electrons spend most of their time equally on the three basal carbons and very little time is spent on the nitrogen. The 5·4 G splitting is probably due to the three possible ^{13}C atoms neighbouring the substitutional nitrogen.

The allowed states for two electrons in an e state are $^1A_1$, ^1E and $^3A_2$. From the optical measurements it is known that the $^1A_1$ is the ground state and that the ^1E state is the lowest lying excited singlet state and it is therefore the $^3A_2$ excited triplet state that is responsible for the ESR signals. An energy level diagram suggested by Loubser and van Wyk (1977) of the lower electronic states is shown in figure 14. The occurrence of the normally forbidden transition from the excited singlet to the triplet state is due to spin–orbit coupling and the theory of the role of spin–orbit coupling in the intersystem crossing of electronic states has been discussed by authors such as Hameka (1967), Hutchison (1967), etc. The reason for the inversion of the spin population is the fact that total symmetry must be preserved in the crossing and that due to this only one of the levels in the triplet system will have the correct symmetry and only it will thus be populated. In this case Loubser and van Wyk (1977) showed that only crossings to levels having some $|T_z\rangle$ character seem to be allowed where $|T_z\rangle$ is one of the zero-field wavefunctions, $|T_x\rangle$, $|T_y\rangle$ and $|T_z\rangle$ of the triplet system. (These wavefunctions describe the three orthogonal possibilities in which the electron spins are in the *yz*, *xz* and *xy* planes, respectively.) This could be deduced from the fact that the high-field lines were always in emission irrespective of the field being parallel or perpendicular to the defect axis. Similar inversion of the high-field ESR line has been observed at helium temperatures in other systems (Si-G9 (Watkins 1967), M-like centre in CaO (Tanimoto *et al* 1965), photo-excited triplet in naphthalene (Schwoerer and Sixl 1969) and Si–S centre (Brower 1971)).

The peaks in the intensity of the ESR signal measured as a function of the wavelength of the exciting light coincided very well with the zero-phonon and phonon-assisted peaks of the 638 nm optical absorption band.

After annealing to 1000 °C the W15 centre got slightly weaker and van Wyk and Loubser (1978) observed the centres W16, W17, W18 and W19. The major principal axis of all centres lay in a {110} plane, and except for W18 all were close to a ⟨111⟩ axis (W19 was 15° away). W17 was the only centre which did have one of its minor principal axes parallel to a ⟨110⟩ axis. Parameter values for these centres are given in table 7. These centres are probably due to defect-impurity complexes.

W20 is a $S=\frac{1}{2}$ centre observed at 77 K after electron irradiation and annealing at 400 °C.

5. Centres due to mechanical deformation

Two processes of mechanical deformation will be discussed. They are grinding and crushing of the material resulting in a fine grain powder, and secondly plastic deformation of single crystals.

In the last twenty years there have been numerous reports of the observation in silicon of an electron spin resonance corresponding to a g of $2{\cdot}0055 \pm 0{\cdot}001$. This resonance is observed in powdered samples, in crystals damaged by polishing or heavy-dose ion implantation, and in evaporated or sputtered amorphous films. It has been proposed that in all these cases the ESR originates from surface dangling bonds either at the external surfaces of the specimen or, in the case of amorphous

material, at the surface of internal voids. However, it is now generally considered to have its origin either from amorphous regions produced by the damage induced in the powdering process (Kaplan *et al* 1975) or from electrons trapped in atomic mis-match regions in the bases of micro-cracks on the surface (Lemke and Haneman 1975).

5.1. Defects in diamond due to grinding

Walters and Estle (1961) were the first to report an ESR signal from crushed diamond. The single line had a g value of $2{\cdot}0027 \pm 0{\cdot}0008$ and had a width of 5–6 G. Schlössin *et al* (1966) found that the intensity of the line increased with decreasing particle size and seemed to saturate as the particle size became smaller than a critical size. It did not decay with time or exposure to water vapour or air as did the signal in powdered quartz. The number of free spins was estimated to be $9{\cdot}5 \times 10^{11}$ cm^{-2} for particles of mean diameter of 72 μm. They interpreted this signal to be due to the Beilby or amorphous layer on the surface of the grains.

Loubser (1977) found two more centres in very fine diamond powders (0·5 μm to 30 μm diameter). The one centre turned out to be the O1 centre seen before in irradiated and annealed single crystals of natural diamond (see §4.3.3 and table 5). A plot of line intensity against the reciprocal of the diameter gave a straight line going through the origin and this indicates that it is indeed a surface phenomenon. The grinding seems to have created vacancies and also to have heated the diamond grains at impact to temperatures of over 500 °C to cause annealing to such an extent that a row of four vacancies could be formed, the model for the O1 centre.

The other centre proved to be the W8 centre observed by Loubser and van Ryneveld (1966) in synthetic diamond grown from a Ni–Fe melt. This centre has been described in §3.3.2. A plot of intensity against particle size shows a variation of the form:

$$\text{Intensity} \propto \frac{(R-a)^2}{R^3}$$

where the best fit was obtained with a value of $a \simeq 0{\cdot}5$ μm. This is interpreted by Loubser (1977) to indicate that the spins causing the signal did not lie on the surface of the particle but on a surface a distance $\simeq 0{\cdot}5$ μm below the true surface. In particles smaller than 0·5 μm the line was virtually absent.

5.2. Defects due to plastic deformation

The W7 centre described first by Loubser and Wright (1973a) has been interpreted by Shcherbakova *et al* (1975) as being due to plastic deformation. It is well-known that plastic deformation in a crystal takes place by the translational slip of dislocations. In case of slip in the ⟨111⟩ plane, when a dislocation 'penetrates' an N1 centre, one of the nitrogen atoms may be displaced relative to the other in the ⟨110⟩ direction by a distance equal to the Burgers vector $(1/\sqrt{2})\,a$. The new N_1CCN_2 impurity centre may lose an electron and become paramagnetic. Diamonds containing this W7 centre are brown in colour with an optical absorption band starting in the region of 0·3 eV and continuing up to 5·5 eV. This band agrees well with the absorption band theoretically predicted for edge dislocations by Bonch-Bruevich and Glasko (1961).

6. Defects introduced by ion implantation in diamond

Ion implantation has become important as it promises to be superior to diffusion techniques as a means for device fabrication. It is also a tool for basic research but the study of the defects produced by ion implantation plays an important role in the final characteristics of the annealed implanted layers. Very little work has been done in the case of diamonds where doping by thermal diffusion does not seem possible. Brosious *et al* (1974a) were the first to use ESR to study ion-implanted diamonds. They used type IIa diamonds and implanted it with boron, carbon and nitrogen ions. When the ions are implanted at room temperature an isotropic line of Lorentzian lineshape and width of ~ 7 G with a g value near the free-electron value is the only feature in all the implanted diamonds for ion fluxes in the range 10^{14}–10^{16} ions cm^{-2} and ion energies in the range 1–3 MeV. This suggests, by comparison with silicon (Title *et al* 1970), that an amorphous layer is formed having a large number of randomly oriented broken bonds at internal surfaces of highly disordered regions. Similar spectral features are observed when diamond surfaces are ground or graphitised (Walters and Estle 1961). There is a general trend of increasing lattice damage as the atomic number of the implanted ion increases.

Annealing studies of the single isotropic line showed regions of reverse annealing at about 100 °C and 400 °C for the ^{14}N implant, 400 °C for the ^{11}B implant and 100 °C and 400 °C for the ^{12}C implant and a rapid drop after this with nearly identical slopes in the range 400–800 °C. Konorova *et al* (1970) also observed a sharp decrease in conductivity approaching the value typical for undoped diamond after annealing to 800 °C. About 95% of the initial damage annealed at 1400 °C. Thus Brosious *et al* came to the conclusion that there is apparently large defect mobility in the range 800 °C to 1000 °C but that some damage still remains similar to neutron-irradiated samples.

Morhange *et al* (1975) implanted type IIa diamonds with 70 keV carbon, nitrogen and boron ions and recorded the defect formation by ESR, optical absorption, luminescence and Raman scattering measurements. They observed the same isotropic line as Brosious *et al* (1974a) but also observed a variation in linewidth with the implantation dose. This seems to indicate that the large linewidth for small doses is due to the superposition of spectra due to different kinds of point defects, while at high doses, when the amount of disorder has saturated, the linewidth is decreased because the spectrum comes only from one source which the authors presumed to be dangling bonds. The intensity of the ESR signal saturates at doses of about 10^{16} cm^{-2}. The density of spins is then of the order of 10^{17} cm^{-3}. This suggests that highly disordered regions, which are created by each impinging ion, overlap when the dose is large enough and form a continuous layer. Morhange *et al* found similar annealing behaviour as Brosious *et al* (1974a).

Brosious *et al* (1974b) found that if the nitrogen ions are implanted at high temperatures ($\simeq 600$ °C) the spectra appear to be a superposition of two signals. One is the line observed at room-temperature implantation, while the other is due to a centre A4, which they interpreted as being due to a $S=1$ state with small D value and $\langle 111 \rangle$ symmetry.

7. Correlation between optical and ESR centres

It is possible to construct models of both impurity defects as well as radiation-induced defects purely from optical absorption measurements or, as has been illus-

trated, from ESR measurements only. The combination of optical, paramagnetic and other techniques, however, produces a powerful combination of complementary data in the light of which a particular model can be rigorously checked. Several cases where such a procedure has been successful will now be discussed.

7.1. The W15 and the 638 nm optical band

The optical and ESR work done on the W15 centre observed in irradiated type Ib diamond after annealing to above 600 °C has already been discussed in §4.4.1 (Loubser and van Wyk 1977, Davies and Hamer 1976). The ESR measurements showed that an excited triplet state becomes populated when illuminated with light of wavelength 638 nm, while the optical measurements showed a $^1A_1 \rightarrow {}^1E$ transition to be responsible for the absorption band. A simple LCAO one-electron molecular orbital calculation showed that a nitrogen-vacancy pair with two electrons in an e orbital gave allowed states $^1A_1$, ^1E and $^3A_2$. A logical assumption is that the electron was somehow excited into the fairly long-lived $^3A_2$ state to give an ESR spectrum characteristic of a triplet. The intersystem crossing from a ^1E to the $^3A_1$ which is normally forbidden is a well-known phenomenon and is made possible by spin–orbit coupling.

7.2. The P2 ESR centre and the N3 optical absorption band at 415 nm

The correlation between the ESR centre P2 and the optical centre N3 which gives some diamonds their yellow colour has been a topic of research and discussion for quite some time (Walter 1891, Bhagavantam 1930, John 1931, Nayar 1941a, Clark *et al* 1956, Sobolev *et al* 1964, Loubser and Wright 1973b). Nayar (1941b) formulated the essential model as some characteristic structural defect in diamond and proposed that the absorption of light occurs by exciting the electrons localised at this defect from one well-defined electronic energy state to another. Clark *et al* (1962) deduced from polarisation of luminescence measurements that this centre, which they called the N3 centre, is aligned along ⟨111⟩ axes and that the transitions occur between a non-degenerate electronic state and one that is doubly degenerate. Uniaxial stress measurements (Runciman 1965, Crowther and Dean 1967) established that the non-degenerate state is the lower. An N2 optical absorption band which absorbs light of 485 nm correlates with the N3 band (Clark *et al* 1956) but the N2 is not a simple absorption band since it has no zero-phonon line.

The P2 ESR spectrum was investigated further by Loubser (1977) and he found that at 77 K an underlying broad line, which was also observed at room temperature, grew in intensity when illuminated with light of wavelength about 420 nm and that this increase could be quenched again by light of lower energy. He proposed a level scheme as shown in figure 15 where there is an intersystem crossing between the excited ^2E and $^2A_1$ states. This $^2A_1$ state will be long-lived as normally no dipole transitions from the vibrational ground state of the electronic state $^2A_2$ to the ground $^2A_1$ state is allowed, while the lifetime of the ^2E state will be very short as fluorescence de-excitation will occur.

Davies *et al* (1978) have done further measurements and found that both the P2 spectrum and the broad line correlate with the 415 nm optical band. They suggest therefore that the broad ESR line is due to absorption in the excited $^2A_2$ state and the P2 ESR lines arise from the $^2A_1$ ground state. The N2 optical band arises from forbidden transitions from the $^2A_1$ to the $^2A_2$ state. Electronic plus vibrational excitation from

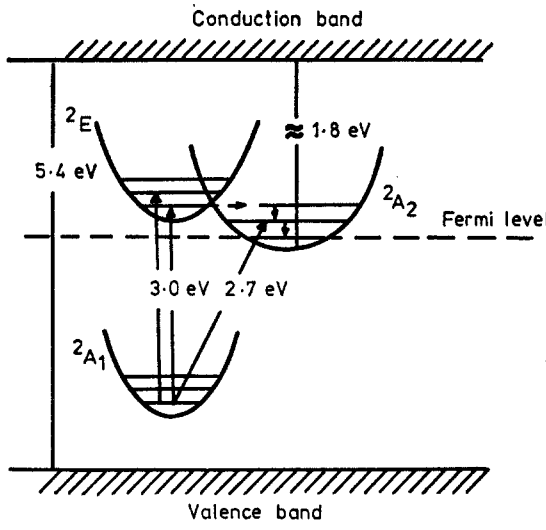

Figure 15. The proposed energy-level diagram of the lower electronic states of the P2 centre shown are the allowed optical transitions from the ground state $^2A_1$ to the ^2E excited state (the N3 absorption band at 3 eV (415 nm)) and the 'forbidden' transitions $^2A_1 \rightarrow {}^2A_2$ (the N2 optical absorption bands at 2·7 eV). The P2 spectrum arises from electrons in the ground state while the single broad line (the N2 ESR line) arises when the electrons are in the $^2A_2$ excited state.

the $^2A_1$ to the excited vibrational levels of the $^2A_2$ electronic state will occur as this state is very similar in energy to the ^2E state and the vibrations will mix the ^2E and $^2A_2$ states and make transitions possible. No zero-phonon line will, however, be excited.

Finally, the model of this centre proposed by Loubser and Wright (1973b) agrees with the Stark effect measurements of Kaplyanskii *et al* (1970) who demonstrated that the N3 optical centre does not possess a centre of inversion. The centre cannot be a pair of impurity atoms substituting for two neighbouring carbon atoms but could be three substitutional impurity atoms bonded to a common atom as this centre would have ⟨111⟩ symmetry without inversion.

It should be mentioned here that Sobolev *et al* (1964) described a correlation between the intensities of the infrared band at 1370 cm^{-1} (the B system) and the P2 centre but later (Sobolev *et al* 1964) found that the correlation was of a purely statistical nature. They did find a correlation with the 415 nm optical band if the broad underlying ESR line—the N2—was taken into account.

7.3. The ND1 optical system and the S1 ESR line

Dyer and du Preez (1965) discovered an optical centre, the ND1, in irradiated type Ib diamonds at 3·6 eV but not irradiated type II diamonds. They also observed an ESR line at $g \simeq 2$, of width 1·9 G. They suggested that this line could be the A, B and C lines reported by Baldwin (1963) and here it is suggested to be the S1 system (see §4.3.1).

This ESR line and the ND1 optical absorption show strikingly similar cyclic behaviour when the diamonds are subjected to alternate heating and optical bleaching cycles. In one diamond, however, they observed a decrease in the ESR signal and an

increase in the ND1 absorption after a 500 °C anneal. Davies (1977) proposes that the ND1 is a negatively charged vacancy and that the cyclical behaviour during heat and light treatment between the GR1 and the ND1 system (Dyer *et al* 1965) can be explained by the capturing of an electron (or a hole) at the same centre. Conversion of the GR1 (V^0) to ND1 (V^-) by blue light (23 250 $cm^{-1} < h\nu < 25\,400$ cm^{-1}) is then seen to be by hole emission ($V^0 \rightarrow V^- + h^+$) explaining the photoconductivity observed by Vermeulen *et al* (1975). The role of the paramagnetic nitrogen is to convert the vacancies produced by irradiation from V^0 to V^- by charge transfer from the nitrogen donors.

However, the S1 ESR line decreases in intensity when the diamond is illuminated with red light (9200 $cm^{-1} < h\nu < 23\,250$ cm^{-1}) (Baldwin 1963). Thus a more detailed study of the optical behaviour of the S1, S2, S3 and S4 lines must be made before a definite pronouncement can be made about which of the lines is associated with the ND1 optical absorption.

7.4. Optical and infrared absorption due to the P1 centre

Dyer *et al* (1965) found that type Ib diamonds exhibited optical absorption in the form of a long tail stretching from about 2·4 eV to about 3·0 eV where the diamond became opaque. In the infrared spectrum two additional features were observed in the two-phonon absorption region, between 7 μm and 9 μm. A strong broad peak at 0·140 eV and a small sharp peak at 0·167 eV seemed to correlate qualitatively with type Ib diamonds. These features were also seen by Charette (1961) in synthetic diamonds which are usually strongly type Ib.

Loubser (1977) found that light of energy larger than 1·8 eV and smaller than 2·3 eV enhances the ESR spectrum of P1 in type Ib diamonds at 77 K but light of higher energies quenched the resonance again. A hysteresis effect was observed; reducing the energy of the light to less than 1·8 eV did not quench the ESR lines. These measurements suggest that the isolated nitrogen centre is normally partially compensated and acts as an acceptor. Shining light of energy of higher than 1·8 eV ionises the centre, the electron being trapped by other trapping centres in the diamond, thus accounting for the increase in ESR signal.

8. Summary and suggestions for further work

The variety of nitrogen centres that have been observed and the scarcity of centres due to other types of impurities may lead one to the conclusion that nitrogen is the only substitutional impurity in diamond. Oxygen may also play a role but it will not show up in an ESR experiment as it has no nuclear moment. The suggested models for most of the nitrogen centres should be tested by uniaxial stress experiments but these experiments will be difficult to perform due to the hardness of the diamond. Diamond seems to be an ideal substance for relaxation measurements as the lines are usually very narrow and saturate very easily. The beautiful cross-relaxation experiment of Sorokin *et al* (1960) is proof of this.

The main conclusion that one can make from the irradiation damage experiments is that impurities play a vital role in the formation of the observed defects. Even in type IIa diamonds, where an impurity estimate of 20 parts per million seems reasonable, most of the centres seem to be associated with impurities. Until purer single

crystals of synthetic diamonds with no magnetic inclusions can be made, this will remain a serious problem.

More low-temperature irradiation experiments should be done on various types of diamond in order to track down the elemental defects. The effect of light of various wavelengths on the intensities and appearance of ESR lines should be extended, as little knowledge of where the impurity levels lie in the forbidden gap has so far been forthcoming.

References

Abragam A and Bleaney B 1970 *Electron Paramagnetic Resonance of Transition Ions* (Oxford: Clarendon Press) chap 9

Abragam A and Pryce M H L 1951 *Proc. R. Soc.* A **205** 135–53

Atkins P W and Symons M C R 1967 *The Structure of Inorganic Radicals* (Amsterdam: Elsevier) p21

Austin I G and Wolfe R 1956 *Proc. Phys. Soc.* B **69** 329–38

Bagdasaryan V S, Markosyan E A, Matosyan M A, Torosyan O S and Sharoyan E G 1975 *Sov. Phys.–Solid St.* **17** 991

Baldwin J A 1963 *Phys. Rev. Lett.* **10** 220–2

Bell M D and Leivo W J 1967 *J. Appl. Phys.* **38** 337–9

Bezrukov G N, Butuzov V P, Gerasimenko N N, Lezheiko L V, Litvin Yu A and Smirnov L S 1970 *Sov. Phys.–Semicond.* **4** 587

Bhagavantam S 1930 *Ind. J. Phys.* **5** 169

Bleaney B 1951 *Phil. Mag.* **42** 441–58

Bloembergen N, Shapiro S, Pershan P S and Artman J O 1959 *Phys. Rev.* **114** 445–59

Bonch-Bruevich V L and Glasko V B 1961 *Sov. Phys.–Solid St.* **3** 26–33

Bourgoin J C, Brosious P R, Kim Y M, Corbett J W and Chrenko R M 1972 *Phil. Mag.* **26** 1167–78

Bower H J and Symons M C R 1966 *Nature* **210** 1037–8

Bratashevskii Yu A, Bukhanko F N, Samsonenko N D and Shapiro O Z 1972 *Sov. Phys.–Solid St.* **13** 1809–10

Brophy J J 1955 *Phys. Rev.* **99** 1336–7

Brosious P R, Corbett J W and Bourgoin J C 1974a *Phys. Stat. Solidi* a **21** 677–83

—— 1977 *J. Physique* **38** 459–62

Brosious P R, Lee Y H, Corbett J W and Cheng L J 1974b *Phys. Stat. Solidi* a **25** 541–9

Brower K L 1971 *Phys. Rev.* B **4** 1968–82

Charette J J 1961 *J. Chem. Phys.* **35** 1906–7

Chrenko R M 1973 *Phys. Rev.* B **7** 4560–7

Clark C D, Ditchburn R W and Dyer H B 1956 *Proc. R. Soc.* A **237** 75–89

Clark C D, Duncan I, Lomer J N and Whippey P W 1964 *Proc. Br. Ceramic Soc.* **1** 85–92

Clark C D, Maycroft G and Mitchell E W J 1962 *J. Appl. Phys.* **33** 378–82

Clark C D and Mitchell E W J 1977 *Radiation Effects in Semiconductors. Inst. Phys. Conf. Ser. No 31* (London: Institute of Physics) pp45–57

Clark C D and Walker J 1973 *Proc. R. Soc.* A **334** 241–57

Collins A T and Williams A W S 1971 *J. Phys. C: Solid St. Phys.* **4** 1789–800

Cook R J and Whiffen D H 1966 *Proc. R. Soc.* A **295** 99–106

Corbett J W 1966 *Solid St. Phys. Suppl. 7*

Corbett J W and Bourgoin J C 1975 *Point Defects in Solids* vol 2, ed J H Crawford and L M Slifkin (New York: Plenum) pp1–149

Coulson C A 1952 *Valence* (Oxford: Oxford University Press)

Coulson C A and Kearsley M J 1957 *Proc. R. Soc.* A **241** 433–54

Coulson C A and Larkins F P 1969 *J. Phys. Chem. Solids* **30** 1963–72

Crowther P A and Dean P J 1967 *J. Phys. Chem. Solids* **28** 1115–36

Davies G 1977 *Nature* **269** 498–500

Davies G and Hamer M F 1976 *Proc. R. Soc.* A **348** 285–98

Davies G, Welbourn C M and Loubser J H N 1978 *Diamond Research* 23–30
Douglas I N and Runciman W A 1977 *J. Phys. C: Solid St. Phys.* **10** 2253–9
Dreybrodt W 1967 *Phys. Stat. Solidi* a **21** 99–112
Duncan I 1965 *Proc. 7th Int. Conf. on Physics of Semiconductors* ed P Baruch (Paris: Dunod) pp135–42
du Preez L 1965 *Thesis* University of the Witwatersrand
Dyer H B and du Preez L 1965 *J. Chem. Phys.* **42** 1898–906
Dyer H B, Raal F A, du Preez L and Loubser J H N 1965 *Phil. Mag.* **11** 763–74
Every A G 1963 *Thesis* University of the Witwatersrand
Every A G and Schonland D S 1965 *Solid St. Commun.* **3** 205–7
Faulkner E A and Lomer J N 1962 *Phil. Mag.* **7** 1995–2002
Faulkner E A, Whippey P W and Newman R C 1965 *Phil. Mag.* **12** 413–4
Feher G 1956 *Phys. Rev.* **103** 834–5
Feher G, Hensel J C and Gere E A 1960 *Phys. Rev. Lett.* **5** 309–11
Friedel J, Lannoo M and Leman G 1967 *Phys. Rev.* **164** A1056–69
Gouterman M and Moffitt W 1959 *J. Chem. Phys.* **30** 1107–8
Griffiths J H E, Owen J and Ward I M 1955 *Rep. Conf. Defects in Crystalline Solids* (London: Phys. Soc.) pp81–7
Hagston W E 1970 *J. Phys. C: Solid St. Phys.* **3** 791–805
Hameka H F 1967 *The Triplet State* ed A B Zahlan (Cambridge: Cambridge University Press) pp1–45
Harris E A, Owen J and Windsor C 1963 *Bull. Am. Phys. Soc.* **8** 252
Hoffman R 1963 *J. Chem. Phys.* **39** 1397–412
Huggins C M and Cannon P 1962 *Nature* **194** 829–30
Hutchison C A 1967 *The Triplet State* ed A B Zahlan (Cambridge: Cambridge University Press) pp63–100
John M V 1931 *Ind. J. Phys.* **6** 305–8
Kaiser W K and Bond W L 1959 *Phys. Rev.* **115** 857–63
Kaplan D, Lépine D, Petroff Y and Thirry P 1975 *Phys. Rev. Lett.* **35** 1376–82
Kaplyanskii A A, Kolyshkin V I and Medvedev V N 1970 *Sov. Phys.–Solid St.* **12** 1193–5
Kim Y M, Lee Y H, Brosious P and Corbett J W 1973 *Radiation Damage and Defects in Semiconductors. Inst. Phys. Conf. Ser. No 16* (London: Institute of Physics) pp202–9
Kim Y M and Watkins G D 1971 *J. Appl. Phys.* **42** 722–4
Klingsporn P E, Bell M D and Leivo W J 1970 *J. Appl. Phys.* **41** 2977–80
Kohn W and Luttinger J M 1955 *Phys. Rev.* **98** 915–22
Konorova E A, Sergienko V F, Vavilov V S, Ershova L M, Kisseleva K V, Krasnopevtsev V V and Milutin Yu V 1970 *Crystal Lattice Defects* **1** 269–74
Larkins F P 1971a *J. Phys. C: Solid St. Phys.* **4** 3065–76
—— 1971b *J. Phys. C: Solid St. Phys.* **4** 3077–82
Leivo W J and Smoluchowski R 1955 *Phys. Rev.* **98** 1532
Lemke B P and Haneman D 1975 *Phys. Rev. Lett.* **35** 1379–82
Lightowlers E C and Collins A T 1966 *Phys. Rev.* **151** 685–8
Lomer Jenifer N and Welbourn C M 1977a *Radiation Effects in Semiconductors. Inst. Phys. Conf. Ser. No 31* (London: Institute of Physics) pp339–45
—— 1977b to be published
Lomer Jenifer N and Wild A M A 1971 *Phil. Mag.* **24** 273–8
—— 1973 *Radiation Effects* **17** 37–44
Loubser J H N 1975 *Diamond Conference, Cambridge* (Johannesburg: De Beers Industrial Diamond Division)
—— 1977 *Solid St. Commun.* **22** 767–70
Loubser J H N and du Preez L 1965 *Br. J. Appl. Phys.* **16** 457–62
Loubser J H N and van Ryneveld W P 1966 *Nature* **211** 517
—— 1967 *Br. J. Appl. Phys.* **18** 1029–31
Loubser J H N, van Ryneveld W P and du Preez L 1965 *Solid St. Commun.* **3** 307–9
Loubser J H N and van Wyk J A 1977 *Diamond Research* 11–4
Loubser J H N and Wright A C J 1973a *J. Phys. D: Appl. Phys.* **6** 1129–41
—— 1973b *Diamond Research* 16–20
Low W 1960 *Solid St. Phys. Suppl. 2*
Ludwig G W and Woodbury H H 1962 *Solid St. Phys.* **13** 223–86

McNeil D A C and Symons M C R 1977 *J. Phys. Chem. Solids* **38** 397–400
Messmer R P and Watkins G D 1970 *Phys. Rev. Lett.* **25** 656–9
—— 1973a *Radiation Damage and Defects in Semiconductors. Inst. Phys. Conf. Ser. No 16* (London: Institute of Physics) pp255–61
—— 1973b *Phys. Rev.* B **7** 2568–90
Mitchell E W J 1965 *Physical Properties of Diamond* ed R Berman (Oxford: Clarendon Press) chap 15
Morhange J F, Beserman R and Bourgoin J C 1975 *Jap. J. Appl. Phys.* **14** 544–8
Nayar P G N 1941a *Proc. Ind. Acad. Sci.* A **13** 534–42
—— 1941b *Proc. Ind. Acad. Sci.* A **14** 1–17
Owen J 1965 *Physical Properties of Diamond* ed R Berman (Oxford: Clarendon Press) chap 10
Pake G E 1962 *Paramagnetic Resonance* (New York: Benjamin)
Podzyarei G A and Zaritskii I M 1968 *Teor. Eksp. Khim.* **4** 281–3
Poole C P 1967 *Electron Spin Resonance* (New York: Wiley)
Ramsey N F 1953 *Nuclear Moments* (New York: Wiley)
Runciman W A 1965 *Proc. Phys. Soc.* **86** 629–36
Samsonenko N D 1965 *Sov. Phys.–Solid St.* **6** 2460–2
Schlössin H H, van Ryneveld W P and Harris W F 1966 *Proc. 1st Congr. Int. Soc. on Rock Mechanics* (Lisbon: Int. Soc. Rock Mechanics) pp119–20
Schwoerer N and Sixl H 1969 *Z. Naturf.* **24a** 952–67
Sellschop J P F, Bibby D M, Erasmus C S and Mingay D W 1974 *Diamond Research* 43–50
Shcherbakova M Ya, Sobolev E V and Nadolinnyi V A 1972 *Sov. Phys.–Dokl.* **17** 513–6
Shcherbakova M Ya, Sobolev E V, Nadolinnyi V A and Aksenov V K 1975 *Sov. Phys.–Dokl.* **20** 725–8
Shcherbakova M Ya, Sobolev E V, Samsonenko N D and Aksenov V K 1969 *Sov. Phys.–Solid St.* **11** 1104–6
Shcherbakova M Ya, Sobolev E V, Samsonenko N D, Nadolinnyi V A, Schastnev P V and Semenov A G 1971 *Sov. Phys.–Solid St.* **13** 281–5
Shul'man L A and Podzyarei G A 1965 *Teor. Eksp. Khim.* **1** 830–3
—— 1972 *Sov. Phys.–Solid St.* **14** 1521–6
—— 1975 *Sov. Phys.–Solid St.* **16** 1377–8
Shul'man L A, Zaritskii I M and Podzyarei G A 1967 *Sov. Phys.–Solid St.* **8** 1842–5
Shul'man L A, Zaritskii I M and Tikhonenko K A 1968 *Sov. Phys.–Solid St.* **9** 1545–8
Smith M J A and Angel B R 1967 *Phil. Mag.* **15** 783–96
Smith M J A, Angel B R and Emmons R G 1966 *Nature* **210** 692–4
Smith W V, Gelles I L and Sorokin P P 1959a *Phys. Rev. Lett.* **2** 39–40
Smith W V, Sorokin P P, Gelles I L and Lasher G J 1959b *Phys. Rev.* **115** 1546–52
Sobolev E V, Bokii G B, Dvoryankin V F and Samsonenko N D 1964 *Zh. Strukt. Khim.* **5** 557–61
Sorokin P P, Lasher G J and Gelles I L 1960 *Phys. Rev.* **118** 939–45
Stoneham A M 1971 *Radiation Effects in Semiconductors* ed J W Corbett and G D Watkins (London: Gordon and Breach) pp7–13
Sturge M D 1967 *Solid St. Phys.* **20** 91–211
Szendrei T 1971 *Solid St. Commun.* **9** 313–4
Tanimoto D H, Ziniker W M and Kemp J O 1965 *Phys. Rev. Lett.* **14** 645–7
Title R S, Brodsky M H and Crowder B L 1970 *Proc. 10th Int. Conf. on Physics of Semiconductors* ed S P Keller, J C Hensel and F Stern (Oak Ridge: USAEC) pp794–8
Urusovskaya A A and Orlov Yu A 1964 *Dokl. Akad. Nauk SSSR* **154** 1099
van Vleck J H 1948 *Phys. Rev.* **74** 1168–83
van Wyk J A and Loubser J H N 1978 to be published
van Wyk J A, Loubser J H N and Welbourn C M 1978 to be published
Vermeulen L A, Clark C D and Walker J 1975 *Lattice Defects in Semiconductors. Inst. Phys. Conf. Ser. No 23* (London: Institute of Physics) pp294–300
Walker J, Vermeulen L A and Clark C D 1974 *Proc. R. Soc.* A **341** 253–66
Walter B 1891 *Ann. Phys. Chem.* **42** 505–10
Walters G K and Estle T L 1961 *J. Appl. Phys.* **32** 1854–9
Watkins G D 1962 *J. Phys. Soc. Japan* **18** *Suppl. II* 22–7
—— 1965 *Proc. 7th Int. Conf. on Physics of Semiconductors* ed P Baruch (Paris: Dunod) pp97–113

Watkins G D 1967 *Phys. Rev.* **155** 802–15
—— 1975 *Point Defects in Solids* vol 2, ed J H Crawford and L M Slifkin (New York: Plenum) pp333–91
Watkins G D and Corbett J W 1961 *Phys. Rev.* **121** 1001–14
—— 1964 *Phys. Rev.* **134** A1359–77
—— 1965 *Phys. Rev.* **138** A543–55
Watkins G D and Messmer R P 1970 *Proc. 10th Int. Conf. on Physics of Semiconductors* ed S P Keller, J C Hensel and F Stern (Oak Ridge: USAEC) pp623–9
Watson R E and Freeman A J 1961a *Phys. Rev.* **123** 521–6
—— 1961b *Phys. Rev.* **124** 1117–23
Wedepohl P T 1957 *Proc. Phys. Soc.* B **70** 177–85
Weigel C and Corbett J W 1976 *Z. Phys.* B **23** 233–8
Weigel C, Peak D, Corbett J W, Watkins G D and Messmer R P 1973 *Phys. Rev.* B **8** 2906–15
Welbourn C M 1976 *PhD Thesis* University of Reading
Welbourn C M and Woods G S 1977 *Diamond Conference, Reading* (Johannesburg: De Beers Industrial Diamond Division)
Whippey P W 1972 *Can. J. Phys.* **50** 803–12
Williams A W S, Lightowlers E C and Collins A T 1970 *J. Phys. C: Solid St. Phys.* **3** 1727–35
Yamaguchi T 1962 *J. Phys. Soc. Japan* **17** 1359–83
—— 1963 *J. Phys. Soc. Japan* **18** 368–80
Zaritskii I M, Bratus V Ya, Vikhnin V S, Vishnevskii A S, Konchits A A and Ustintsev V M 1976 *Sov. Phys.–Solid St.* **18** 1883–5
Zavoisky E 1945 *J. Phys. USSR* **9** 245